

Research article

Climate risk assessment at Chinese provinces: A novel Criteria and Context Decomposition for Trade-Off Weighting (CCDTW) approach

Peter Wanke ^a, Yong Tan ^{b,*}

^a Getulio Vargas Foundation, EBAPE–Brazilian School of Public and Business Administration, Rio de Janeiro, Brazil

^b School of Management, University of Bradford, Bradford, West Yorkshire, BD7 1DP, UK



ARTICLE INFO

Keywords:

Climate risk assessment
Multi-criteria decision-making
Chinese provinces
Socio-economic contextual variables
QR decomposition

ABSTRACT

This paper introduces the Criteria and Context Decomposition for Trade-Off Weighting (CCDTW) methodology, a novel multi-criteria decision-making (MCDM) approach for assessing and ranking climate risks across Chinese provinces. Using a non-balanced panel dataset of 1457 observations, the CCDTW integrates QR decomposition to decorrelate climate risk criteria—extreme low and high temperatures, rainfall, and drought—and socio-economic contextual variables, capturing trade-offs and relative importance among them. Weighted trade-off coefficients are derived to construct a Climate Risk Index (CRI), which facilitates the ranking and benchmarking of provinces over time. The results reveal heterogeneous patterns of climate risk across regions, with increasing trends in extreme temperatures and rainfall in recent years. The CRI indicates that employment, power generation, and population access to natural gas are the primary drivers of climate risk, highlighting the trade-offs between economic welfare and climate mitigation. This framework provides policymakers with actionable insights to design region-specific and time-sensitive climate risk management strategies.

1. Introduction

Climate change has emerged as one of the most pressing challenges of the 21st century, with profound implications for ecosystems, economies, and societies (Tol, 2018; Malhi et al., 2020). Its multifaceted impacts manifest in extreme weather events, changing precipitation patterns, and rising temperatures, significantly increasing vulnerabilities across regions (Pandit and Sharma, 2023). In particular, China, as a geographically and economically diverse nation, faces complex climate risks that vary widely across its provinces, necessitating targeted strategies for mitigation and adaptation (Mi and Sun, 2021; Yang et al., 2024).

Addressing these risks requires robust methodologies to assess and rank climate vulnerabilities, enabling policymakers to allocate resources effectively and design region-specific interventions (Ebi et al., 2006). Traditional approaches often focus on isolated indicators, such as economic damages or environmental degradation, without fully capturing the interplay between climate criteria and socio-economic factors (Esperón-Rodríguez et al., 2016). This limitation underscores the need for a comprehensive framework that integrates multiple dimensions of climate risk while accounting for their interdependencies (Dawson,

2015).

In this paper, we propose the **Criteria and Context Decomposition and Trade-Off Weighting (CCDTW)** methodology, a novel multi-criteria decision-making (MCDM) approach for climate risk assessment. By employing QR decomposition, the CCDTW method decorrelates climate risk criteria—such as extreme temperatures, rainfall, and drought—and contextual variables, such as economic activity and energy consumption, to isolate their independent contributions and interactions (Gu and Eisenstat, 1996). Weighted trade-off coefficients are then derived to construct a Climate Risk Index (CRI), which enables the ranking of provinces based on their overall climate vulnerability.

This study focuses on a non-balanced panel dataset of 1457 observations, representing key climate and contextual variables across Chinese provinces. The CCDTW methodology offers several innovations, including the ability to quantify trade-offs among criteria, incorporate contextual drivers into climate risk assessment, and provide actionable insights for policymakers. The results reveal significant temporal and spatial heterogeneities in climate risk, driven by both environmental and socio-economic factors, with implications for regional climate resilience planning. By combining advanced decomposition techniques with a robust weighting scheme, this study contributes to the growing

* Corresponding author.

E-mail address: y.tan9@brad.ac.uk (Y. Tan).

literature on climate risk assessment and offers a practical tool for decision-makers in designing evidence-based climate adaptation strategies.

This paper makes three key contributions: 1) Methodological innovation: We introduce the Criteria and Context Decomposition for Trade-Off Weighting (CCDTW) framework, combining QR-based orthogonal decomposition with trade-off weighting to overcome multicollinearity and capture socio-economic drivers in climate risk assessment; 2) Practical policy insights: By constructing a Climate Risk Index (CRI) for Chinese provinces, we identify the top drivers of vulnerability—employment, power generation, and natural-gas access—and offer region-specific recommendations for targeted adaptation and mitigation strategies; 3) Societal impact: The CCDTW approach equips policymakers, NGOs, and community stakeholders with a transparent, data-driven tool to prioritize investments in infrastructure resilience, energy transition, and community-level adaptation strategies—such as targeted emission-reduction policies, renewable energy deployment, and water-security measures—to reduce the socio-economic vulnerabilities exposed by extreme weather events.

The remainder of the paper is organized as follows: Section 2 provides a comprehensive review of literature on various aspects of climate risk investigation as well as the application of MCDM in risk analysis. Section 3 presents the methodological framework of the CCDTW model. Section 4 provides the analysis and discusses the results of the climate risk assessment, including the spatial and temporal patterns observed across Chinese provinces. Section 5 summarizes the advantages of the proposed approach over other competing methods for ranking climate risks with the MCDM ambit. Section 6 provides conclusions and policy implications, highlighting the utility of the CCDTW framework in addressing climate challenges.

2. Literature review

Climate risk assessment has become increasingly critical for understanding and mitigating the complex impacts of climate change on socio-economic systems. This section reviews relevant literature on the investigation of climate risk, including the socio-economic impacts of climate risk; climate risk and technological innovation; perceptions and values in climate risk management; climate risk assessment through different methods, and MCDM applications in risk analysis.

Recent advances in climate risk research have emphasized the importance of decomposing risk dimensions and understanding their region-specific impacts, particularly in emerging economies. Zhou et al. (2025) introduced an innovative framework combining necessary condition analysis (NCA) and fuzzy set qualitative comparative analysis (fsQCA) to assess the joint effects of climate physical risk (CPR), transition risk (CTR), and economic policy uncertainty on carbon prices in China's provincial carbon markets. Their study demonstrates the significance of spatial heterogeneity in climate risk impacts and supports the move toward localized, data-driven policy tools—an objective shared by the CCDTW model proposed in this study. Similarly, Saqib et al. (2024) examined the influence of physical and transition climate risks on stock market returns across BRICS economies, employing panel-level and country-specific econometric models. Their findings underscore that while transition risks have widespread financial consequences, physical risks exhibit strong country-level variation. Together, these studies highlight both the financial and policy relevance of disaggregated, multi-dimensional climate risk analysis and reinforce the need for subnational, context-sensitive assessment frameworks such as CCDTW to inform targeted adaptation strategies.

Recent advances in the literature have explored how various forms of uncertainty—particularly policy-related—impact the capacity of economies to respond to climate risks through innovation. Attilio (2025) investigates the influence of climate policy uncertainty (CPU) on green innovation across ten economies using a Global Vector Autoregressive (GVAR) model. The study reveals that CPU shocks reduce green

innovation both directly and indirectly, via spillover effects through interconnected economic, geopolitical, and financial channels. By incorporating five dimensions of uncertainty—climate, economic, energy-related, financial, and geopolitical—the analysis demonstrates that green innovation, particularly in technologies related to climate change mitigation and environmental management, is highly sensitive to uncertainty shocks. This work is highly relevant to climate risk assessment frameworks such as the CCDTW proposed in this paper, as it underscores the role of contextual uncertainties in shaping vulnerability and adaptive capacity across regions. Furthermore, Attilio's findings support the inclusion of policy and geopolitical risk variables as influential contextual drivers in climate risk modeling, emphasizing the interdependence between governance stability and technological adaptation outcomes.

Perceptions and values in climate risk management have been widely recognized as critical components shaping local adaptation responses. Andrista et al. (2025) conducted a comprehensive mixed-methods study examining how small-scale farmers across six Indonesian districts perceive climate change and implement adaptive strategies. Their research demonstrates that farmers' perceptions of climate variability—such as changes in rainfall patterns, temperature, and frequency of hazards—play a pivotal role in determining adaptation responses, including crop diversification, land maintenance, and livelihood diversification. Importantly, the study emphasizes the influence of gender, access to government support, and information dissemination on farmers' behavioral responses, highlighting the need for context-sensitive and socially inclusive adaptation policies. The findings underscore that perceptions are not only informed by environmental cues but also shaped by socioeconomic and institutional factors—reinforcing the notion that values embedded in local knowledge systems significantly condition climate risk management outcomes. This aligns with the present study's emphasis on integrating socio-economic contextual variables in climate risk assessment frameworks, supporting the case for subnational, perception-informed metrics like the CCDTW approach.

Sperotto et al. (2017) conducted a comprehensive review of the applicability of Bayesian Networks (BNs) in the context of climate change impacts assessment and risk management, emphasizing a multi-risk perspective. Their study underscores the value of BNs as probabilistic graphical models capable of capturing interdependencies among multiple stressors, representing uncertainty, and supporting scenario-based risk evaluations. The paper identifies key advantages of BNs, including their capacity to integrate diverse sources of data, model cumulative and cascading effects, and enhance stakeholder communication through intuitive visual structures. However, it also acknowledges critical limitations, such as the challenges in representing temporal and spatial dynamics and the difficulty in achieving quantitative validation. These strengths and constraints resonate with the goals of the CCDTW framework developed in the present study, which similarly aims to assess climate risk across multiple dimensions while addressing limitations in traditional mono-causal approaches. While BNs offer a flexible and interpretative framework for qualitative and semi-quantitative risk modeling, the CCDTW approach extends this line of inquiry by incorporating a mathematically rigorous decomposition technique (QR) and trade-off weighting mechanism to disentangle the independent and interacting effects of climate and contextual variables. Thus, Sperotto et al.'s work provides a foundational basis for exploring integrated, adaptive climate risk models, against which more structured, data-driven methods such as CCDTW can be evaluated.

Mohammadifar et al. (2023) proposed a novel hybrid framework that integrates deep learning with ensemble multi-criteria decision-making (MCDM) techniques to assess flood risk in the Minab-Shamil plain of southern Iran. Specifically, their study combined a multiplicative long short-term memory (mLSTM) model for flood hazard prediction with an ensemble of three MCDM methods—CODAS (Combinative Distance-Based Assessment), EDAS (Evaluation Based on Distance from

Average Solution), and MOOSRA (Multi-Objective Optimization on the Basis of Simple Ratio Analysis)—for flood vulnerability assessment. The resulting flood risk map, derived by spatially combining hazard and vulnerability outputs, was shown to offer high predictive accuracy, with performance metrics exceeding 90 % in most validation criteria. Importantly, their use of ensemble MCDM modeling enabled a robust and comparative assessment of vulnerability factors, validated via Spearman's rank correlation, thus improving model consistency. This study exemplifies the integration of MCDM in environmental risk mapping and highlights the utility of combining data-driven learning models with structured decision frameworks. It provides a compelling precedent for incorporating ensemble MCDM approaches into climate risk assessments, supporting the methodological direction of this study's CCDTW framework.

3. Methodology

The Criteria and Context Decomposition and Trade-Off Weighting (CCDTW) model is a novel multi-criteria decision-making (MCDM) framework developed to assess and rank climate risks across Chinese provinces. This approach integrates mathematical decomposition techniques and regression modeling to quantify and rank climate risks across provinces using decorrelated risk criteria; incorporate contextual variables to evaluate their impact on climate risk; establish a weighted trade-off framework to determine the influence of interactions among criteria and contextual variables; and develop a comprehensive Climate Risk Index (CRI) to rank provinces and assess temporal changes in risk patterns.

The advantages of CCDTW over the existing MCDM approaches for score building and benchmarking are threefold. First, the orthogonal decomposition – in this research, as further explained, QR decomposition is adopted – not only reduces multicollinearity among criteria and contextual variables but also helps in isolating independent dimensions of risk and contextual influence. Second, the trade-off weighting allows the incorporation of interdependence and relative importance of criteria and contextual variables, providing a nuanced understanding of climate risk drivers. Third, regression-based weighting is also employed to quantify the direct and weighted impacts of contextual variables on criteria.

The overall motivation for this novel approach is to help decision-makers in (1) designing policies (by the identification of high-risk provinces and prioritized interventions); (2) monitoring temporal trends (by tracking the evolution of climate risks over time); and (3) establishing regional comparisons (by computing risk profiles across provinces to allocate resources efficiently).

Step 1: Orthogonal Decomposition of Criteria and Contextual Variables.

The QR decomposition (Sharma et al., 2013) was applied to the climate risk criteria matrix (A) and the contextual variables matrix (B) to decorrelate the data and isolate independent components.

For the criteria matrix:

$$A = QR \quad (1)$$

where:

Q is an $n \times m$ orthogonal matrix representing decorrelated climate risk criteria.

R is an $m \times m$ upper triangular matrix capturing trade-offs and the relative importance of the criteria.

Readers should note that the off-diagonal elements of R (i.e., r_{ij} for $j < i$) measure the degree of linear dependency between criteria j and i . These elements quantify the projection of one criterion onto the basis vector of another, reflecting a “trade-off” or interaction. A large off-diagonal element (positive or negative) indicates that criterion j depends heavily on criterion i , meaning there is a strong trade-off between them. On the other hand, a zero or near-zero off-diagonal element

implies independence in contribution. Thus, the off-diagonal elements capture the extent to which one criterion's variance substitutes for or interacts with another, hence the term *trade-off*.

For the contextual variables:

$$B = Q_b R_b \quad (2)$$

where:

Q_b is an $n \times p$ orthogonal matrix representing decorrelated contextual variables.

R_b is a $p \times p$ upper triangular matrix capturing trade-offs and the relative importance of contextual variables.

The QR decomposition presents two key properties (Srinivasa, 2012; Zhuang et al., 2024).

Orthogonality of Q and Q_b . The columns of Q and Q_b are orthonormal such as $Q^T Q = I$ and $Q_b^T Q_b = I$. This property ensures that the criteria and contextual variables are decorrelated, enabling a clearer analysis of their individual contributions.

Upper Triangular Structure of R and R_b . The diagonal elements of R and R_b capture the relative magnitudes (importance) of the criteria or contextual variables. On the other hand, the off-diagonal elements capture trade-offs or interactions between criteria or contextual variables.

Step 2: Regression of Criteria onto Contextual Variables.

This step involves quantifying the influence of decorrelated contextual variables (Q_b) on decorrelated climate risk criteria (Q) through ordinary least squares (OLS) regression. The objective is to capture the extent to which each contextual variable explains variation in the criteria, while ensuring that interdependencies among the variables and criteria are minimized due to prior orthogonalization.

The relationship between the decorrelated climate risk criteria (Q) and decorrelated contextual variables (Q_b) is expressed as:

$$Q = Q_b C + \epsilon \quad (3)$$

where:

Q is an $n \times m$ matrix of decorrelated climate risk criteria, where n is the number of observations (provinces and years) and m is the number of criteria (e.g., extreme low temperature days (LTD), extreme high temperature days (HTD), extreme rainfall (ERD), extreme drought days (EDD)).¹

Q_b is an $n \times p$ matrix of decorrelated contextual variables, where p is the number of contextual variables (e.g., energy consumption, population statistics).

C is a $p \times m$ matrix of regression coefficients, representing the impact of contextual variables on each climate risk criterion.

ϵ is an $n \times m$ residual matrix, capturing unexplained variability in the criteria.

The regression coefficients C are estimated using the ordinary least squares formula:

$$C = (Q_b^T Q_b)^{-1} Q_b^T Q \quad (4)$$

where:

$Q_b^T Q_b$ is the $p \times p$ covariance matrix of the contextual variables.

$Q_b^T Q$ is the $p \times m$ cross-covariance matrix between contextual variables and criteria.

The resulting matrix C quantifies how each decorrelated contextual variable influences each decorrelated climate risk criterion. Each element C_{ij} in the matrix C represents the unweighted influence of the

¹ LTD: number of Low-Temperature Days (daily minimum temperature <10th percentile). HTD: number of High-Temperature Days (daily maximum temperature >90th percentile). ERD: number of Extreme-Rainfall Days (daily rainfall >95th percentile). EDD: number of Extreme-Drought Days (daily relative humidity <5th percentile).

i-th contextual variable on the *j*-th climate risk criterion:

Positive C_{ij} : An increase in the *i*-th contextual variable is associated with an increase in the *j*-th climate risk criterion.

Negative C_{ij} : An increase in the *i*-th contextual variable is associated with a decrease in the *j*-th climate risk criterion.

These coefficients form the basis for understanding the relationship between contextual variables and criteria, and they are further refined in Step 3 through weighting.

Step 3: Weighted Trade-Off Coefficients.

The unweighted regression coefficients (C) were adjusted using the trade-off matrices (R and R_b) to account for interdependencies among criteria and contextual variables. The weighted trade-off matrix (CR) was computed as:

$$CR = \frac{R_b}{\max(R_b)} \cdot \frac{C}{\max(C)} \cdot \frac{R}{\max(R)} \quad (5)$$

where:

$R_b/\max(R_b)$: Normalized contextual trade-off matrix, capturing the relative importance of contextual variables.

$C/\max(C)$: Normalized regression coefficients, representing the unweighted influence of contextual variables on criteria.

$R/\max(R)$: Normalized criteria trade-off matrix, capturing the relative importance and interactions of climate risk criteria.

In other words, this formulation integrates the importance and trade-offs among contextual variables ($R_{b,\text{norm}}$); the direct influence of contextual variables on criteria (C_{norm}); the importance and trade-offs among criteria (R_{norm}). Each element CR_{ij} in the matrix CR represents the weighted impact of the *i*-th contextual variable on the *j*-th climate risk criterion:

Positive CR_{ij} : Indicates that the *i*-th contextual variable has a weighted positive impact on the *j*-th criterion, increasing climate risk.

Negative CR_{ij} : Indicates a weighted mitigating effect, reducing the associated climate risk.

Readers should also note that each element cr_{ij} in CR reflects the contextual-adjusted impact of the *i*-th contextual variable on the *j*-th climate criterion, weighted by their respective importance (diagonal) and interaction (offdiagonal) structures. In other words, each element of CR represents the weighted and normalized influence of a contextual factor on a climate criterion, accounting for: its individual contribution (from C); its interaction with other contextual variables (via R_b); and the sensitivity of the criterion to other criteria (via R) in terms of their trade-offs, that is the partial dependencies and substitution patterns among climate risk criteria.

In summary, this step integrates the relative importance of contextual variables and criteria relationships (dependencies and interactions) into the weighting process to produce weighted trade-off coefficients (CR), which serve as the foundation for constructing the Climate Risk Index (CRI) in subsequent steps.

Step 4: Climate Risk Index (CRI).

In Step 4, the weighted trade-off coefficients (CR) from Step 3 are aggregated to compute the Climate Risk Index (CRI) coefficients for each observation. These coefficients serve as an intermediate metric, summarizing the combined impacts of all contextual variables on overall climate risk. The CRI coefficients enable the translation of contextual variable impacts into actionable climate risk insights for ranking and scoring provinces. The goal in Step 4 is to aggregate the CR matrix to produce a single CRI coefficient for each contextual variable. The CRI coefficient for the *i*-th contextual variable is computed as the row sum of the CR matrix:

$$\text{CRI}_i = \sum_{j=1}^m CR_{ij} \quad (6)$$

where:

CR_{ij} is the weighted trade-off coefficient for contextual variable *i* and

criterion *j*.

m is the number of climate risk criteria

Positive CRI values: Indicate that the contextual variable has a net detrimental effect on climate risk (above the median).

Negative CRI values: Indicate that the contextual variable has a net mitigating effect on climate risk (below the median).

The CRI coefficients summarize the overall climate risk contribution of each contextual variable providing a comprehensive risk profile.

Step 5: Application of CRI Coefficients to Generate Climate Risk Scores.

In Step 5, the Climate Risk Index (CRI) coefficients derived in Step 4 can be also applied to the original contextual variables (B) to compute climate risk scores for each observation. This step translates the individual CRI coefficients for each contextual variable into aggregate risk scores for provinces or years, which can be used for comparison, ranking, and policy prioritization.

The climate risk score for the *i*-th observation is computed as a weighted sum of the original contextual variables (B) using the CRI coefficients (CRI):

$$\text{Score}_i = \sum_{j=1}^p \text{CRI}_j \cdot B_{ij} \quad (7)$$

where:

Score_i : Climate risk score for the *i*-th observation (e.g., a province-year combination).

CRI_j : Climate Risk Index coefficient for the *j*-th contextual variable.

B_{ij} : Value of the *j*-th contextual variable for the *i*-th observation.

p : Number of contextual variables

To facilitate interpretation and comparability across observations, the risk scores are normalized using min-max scaling

$$\text{Score}_{\text{norm},i} = \frac{\text{Score}_i - \min(\text{Score})}{\max(\text{Score}) - \min(\text{Score})} \quad (8)$$

where:

$\text{Score}_{\text{norm},i}$: Normalized climate risk score for the *i*-th observation.

$\min(\text{Score})$: Minimum climate risk score across all observations.

$\max(\text{Score})$: Maximum climate risk score across all observations.

Step 6: Temporal and Spatial Analysis.

In Step 6, the normalized climate risk scores computed in Step 5 are regressed against temporal (year) and spatial (province) variables. The objective is to analyze how climate risks evolve over time and vary across provinces, providing critical insights into temporal trends and regional disparities in climate vulnerability.

The normalized climate risk score is modeled as a function of temporal and spatial variables:

$$\text{Score}_{\text{norm},i} = \beta_0 + \beta_1 \cdot \text{Year}_i + \sum_{j=1}^k \gamma_j \cdot \text{Province}_{ij} + \epsilon_i \quad (9)$$

where:

$\text{Score}_{\text{norm},i}$: Normalized climate risk score for observation *i*.

β_0 : Intercept term, representing the baseline climate risk score.

β_1 : Coefficient for the temporal variable (Year), capturing the trend in climate risk over time.

γ_j : Coefficients for the spatial variables (Province_{ij}), representing the deviation in climate risk for province *j* relative to the reference province.

ϵ_i : Residual error term.

k : Number of provinces minus one (reference province is excluded to avoid multicollinearity).

A schematic overview of the entire CCDTW workflow is presented in Fig. 1.

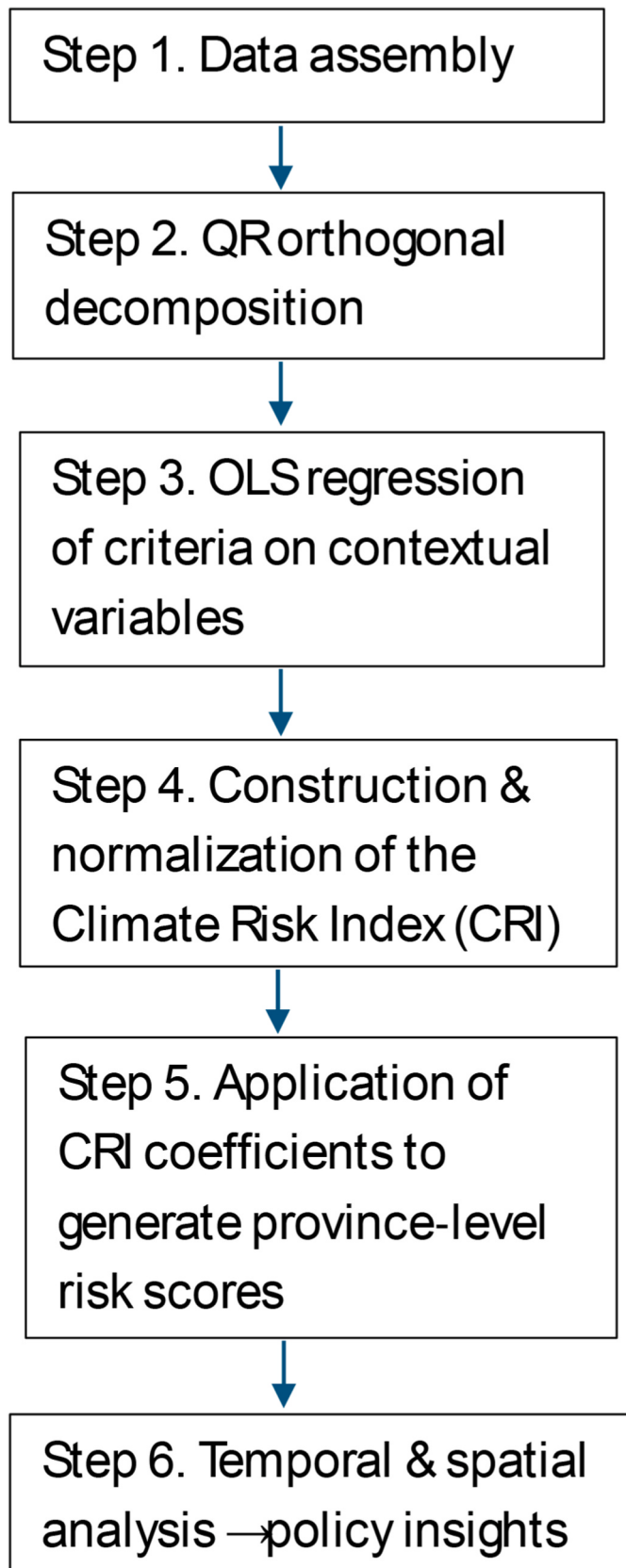


Fig. 1. Research stages of the CCDTW approach.

4. Analysis and discussion of results

Tables 1 and 2 report, respectively, on the descriptive statistics for the four analyzed climate risk criterion index and the socio-economic contextual variables related to them at the provincial level in China. The dataset was obtained from two distinct sources, National Oceanic and Atmospheric Administration (NOAA), Washington, DC, U.S. and National Bureau of Statistics of China, and after merging and cleaning for NA values, a final non-balanced panel comprising 1457 observations was obtained over the period between 2008 and 2019, as described in Table 3, which reports the number of valid observation entries per year, province, and city. A valid observation corresponds to a full record of climate risk criteria and socio-economic contextual variables for a given city in a given year.

We focus on the years 2008–2019 for two reasons. first, this interval spans key policy and environmental milestones in China—most notably the 2008 Sichuan earthquake, the roll-out of its 11th and 12th Five-Year Plans, and the global Paris Agreement in 2015—allowing us to capture how major shocks and policy changes affect climate risk profiles. Second, ending in 2019 ensures our analysis is unaffected by the severe economic disruptions of 2020 and beyond, isolating “baseline” climate–society interactions.

This study focuses on China’s mainland territory, analyzing climate risk across 20 selected provinces using prefecture-level data (i.e. cities and autonomous prefectures within each province). We selected provinces based on a data completeness threshold to ensure the robustness of our Climate Risk Index (CRI) construction. Specifically, we included only those provinces that contained at least 7 prefecture-level units with data for all key climate and socio-economic variables for a substantial portion of the study period (2008–2019). This resulted in a non-balanced panel of 1457 observations across 20 provinces. The selected provinces are: Anhui (84 observations), Beijing (11), Gansu (97), Guizhou (6), Hebei (84), Heilongjiang (108), Henan (84), Hubei (88), Inner Mongolia (132), Jiangsu (24), Jilin (84), Liaoning (96), Ningxia (36), Qinghai (54), Shaanxi (72), Shandong (132), Tianjin (12), Xinjiang (168), Yunnan (45), and Zhejiang (58). The numbers in parentheses refer to the total number of valid province–city–year entries per province, as shown in Table 3. Provinces with insufficient prefecture-level coverage or high rates of missing data were excluded. This selection ensures that the CRI is based on consistent and sufficiently representative data from each region, improving comparability and reliability of the results across diverse geographical, climatic, and economic settings in China. Fig. 2 shows the medium values of the four risk criteria (LTD, HTD, ERD and EDD) at the provincial level over the examined period. More specifically, Fig. 2a shows the medium values of LTD, Fig. 2b shows the medium values of HTD, Fig. 2c shows the medium values of ERD and Fig. 2d shows the medium values of EDD. As can be seen, the maps have been highlighted by three colors, yellow, orange and red, representing low risk, medium risk and high risk, respectively. The provinces’ names and locations have been illustrated in a map in Appendix A, while the medium values of these four risk criteria have been presented in Appendix B.

In their turn, Figs. 3 and 4 report, respectively, on the CCDTW results for the four climate risk indexes median values, as grouped by year and province. After performing the QR decomposition, decorrelated and rescaled metrics for LTD, HTD, ERD, and EDD revealed several results (matrix Q). Specifically with respect to Fig. 4, in order to capture the spatial profile of climate risks, we computed the median of each orthogonalized criterion per province over the 2008–2019 period.

First, while it is not possible to affirm at first sight an increasing trend in median extreme drought and rainfall over the years, it appears that extreme high and low temperatures are spiking, mainly after 2015 and 2012, respectively (cf. Fig. 3). This post-2015 spike in extreme high temperature aligns with global climate change patterns, where rising greenhouse gas emissions have contributed to a consistent increase in average and extreme temperatures. Recent peer-reviewed studies

Table 1

Descriptive statistics for the climate risk criterion indexes.

Criterion	mean	sd	cv	max	min	skewness	kurtosis	entropy
LTD	21.59	8.22	0.38	44.86	0.00	-0.02	-0.64	6.50
HTD	43.96	11.67	0.27	97.30	0.00	0.17	1.41	6.55
ERD	26.99	28.04	1.04	368.75	0.00	4.84	35.82	4.41
EDD	18.34	11.51	0.63	76.87	0.00	1.32	2.55	6.77

● LTD: extreme low-temperature days; HTD: extreme high-temperature days; ERD: extreme rainfall days; EDD: extreme drought days.

Table 2

Descriptive statistics for the contextual variables.

Contextual Variables	mean	sd	cv	max	min	skewness	kurtosis	entropy	unit
Employment	13.444	5.779	0.430	27.900	1.200	0.275	-0.234	6.614	10,000 persons
Output_of_Natural_Gas	57.203	110.619	1.934	473.420	0.000	2.048	2.832	6.667	100 million cubic meters
Power_Generation	2115.935	1255.714	0.593	5897.220	242.650	0.826	0.416	7.486	100 million kwh
Total_Supply_of_Natural_Gas	25.261	22.203	0.879	191.600	2.760	2.228	7.617	7.448	100 million cubic meters
Population_with_Access_to_Gas	865.113	639.107	0.739	3395.000	68.700	1.703	3.330	7.486	10,000 persons
Supply_of_Liquefied_Petroleum_Gas	25.715	23.482	0.913	93.700	0.640	1.201	0.511	7.445	10,000 tons
Population_with_Access_to_Liquefied_Petroleum_Gas	404.872	319.856	0.790	1404.360	12.180	1.164	0.969	7.420	10,000 persons
Hot_water_supply	24,593.909	20,192.298	0.821	123,814.000	2.000	0.517	-0.369	7.299	Mega watts
Coal_Consumption	18,244.150	11,162.450	0.612	49,035.950	276.190	0.765	-0.282	7.486	10,000 tons
Coke_Consumption	1700.910	1865.234	1.097	9371.810	0.010	2.301	5.435	7.486	10,000 tons
Crude_Oil_Consumption	2344.676	2608.203	1.112	13,632.100	0.020	2.219	5.027	7.486	10,000 tons
Gasoline_Consumption	387.207	236.559	0.611	1085.870	18.770	0.461	-0.803	7.475	10,000 tons
Kerosene_Consumption	42.904	53.157	1.239	691.030	0.010	5.508	50.205	7.382	10,000 tons
Diesel_Oil_Consumption	644.675	346.770	0.538	1814.340	78.380	0.852	0.603	7.486	10,000 tons
Fuel_Oil_Consumption	262.699	738.958	2.813	4686.430	0.030	4.204	18.623	7.456	10,000 tons
Natural_Gas_Consumption	57.007	41.428	0.727	288.060	7.170	1.659	3.984	7.462	100 million cubic meters
Electricity_Consumption	1951.904	1251.525	0.641	6264.000	313.230	1.187	1.410	7.486	100 million kwh
Sulfur_Dioxide	64.911	45.686	0.704	182.740	0.270	0.778	-0.457	7.466	10,000 tons
Government_Expense_on_Environment	123.056	77.031	0.626	502.500	10.980	1.826	4.384	7.486	100 million yuan
Civil_Vehicles	503.564	442.590	0.879	2333.730	20.250	1.855	3.606	7.480	10,000 units
Private_Vehicles	427.689	404.779	0.946	2092.390	10.790	1.870	3.588	7.486	10,000 units
Passenger_Traffic	74,380.574	59,438.071	0.799	265,632.000	5602.000	1.428	1.535	7.486	10,000 persons
Freight_Traffic	144,230.399	95,974.202	0.665	434,298.000	9115.000	0.693	-0.180	7.484	10,000 tons
Waste_Gas_Treatment	179,966.119	208,919.937	1.161	1,281,351.000	4515.000	2.594	7.676	7.486	10,000 yuan
Gross_Regional_Product	19,375.698	15,444.686	0.797	98,656.800	896.900	1.617	3.339	7.486	100 million yuan

confirm that 2023 and 2024 were the warmest years on record, marking a globally recognized temperature spike consistent with the broader trajectory of anthropogenic warming (Goessling et al., 2025; Bevacqua et al., 2025; Xie et al., 2025). However, and counterintuitively, global warming can intensify polar vortex events, leading to periods of extreme cold in localized areas. This phenomenon has been observed in regions influenced by shifts in Arctic air masses due to destabilized jet streams, particularly in parts of northern China (Liu et al., 2024).

Fig. 4 shows that despite this partial unbalance in drought events, extreme rainfall appears to be increasing in the majority of the provinces analyzed, regardless of their geographic location. The increasing rainfall trend is consistent with climate models predicting more intense and frequent precipitation events in many parts of the world due to increased atmospheric moisture content from warming oceans (Gu et al., 2023), as well as with observational evidence of intensified spring rainfall in southern China linked to multi-year El Niño events (Zhong et al., 2023).

While Gu et al. (2023) analyze climate risk factors—specifically precipitation anomalies—at the global scale, we draw comparisons based on shared physical trends and broad climatic relevance, not strict geographic or methodological alignment. Although their work does not focus on China specifically, it identifies global shifts in precipitation regimes that are relevant to understanding long-term trends in our provincial-level Climate Risk Index (CRI). We use such references not for direct one-to-one comparability, but to corroborate the general direction and nature of the climate-related impacts we observe. Where possible, we prioritize studies with methodological, contextual, or climatic relevance to China or other monsoonal or rapidly developing regions. The widespread nature of this trend across provinces indicates systemic drivers such as large-scale climatic phenomena (e.g., monsoon intensification or El Niño effects) (Zhong et al., 2023). On the other hand, extreme high temperatures appear to be increasing in Gansu, Ningxia, Qinghai, and Yunnan, while decreasing or remaining steady in Anhui,

Table 3

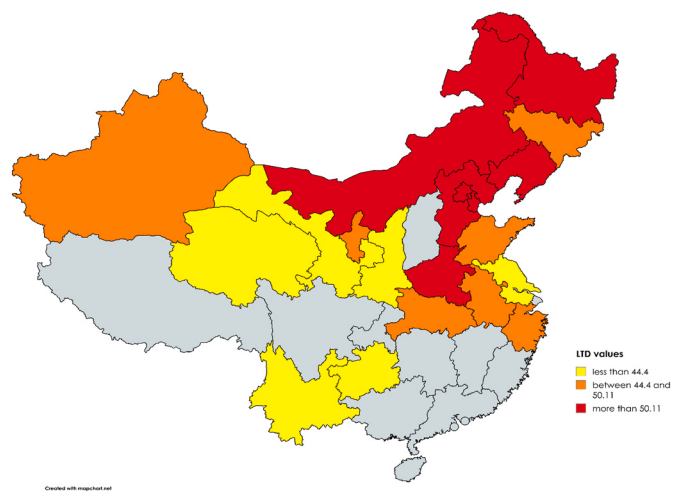
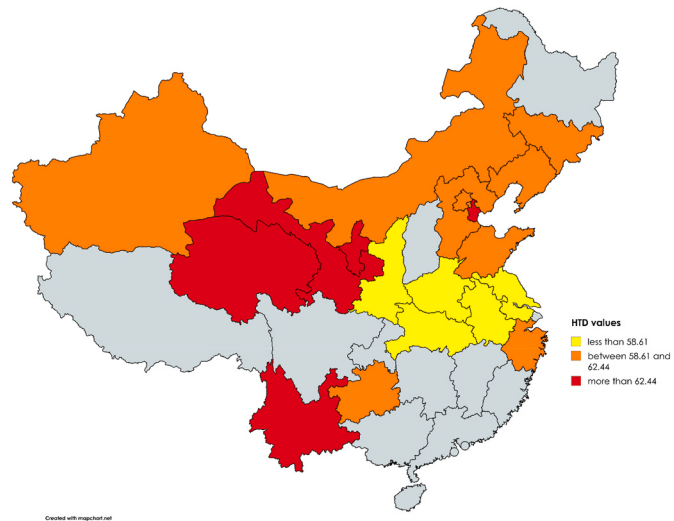
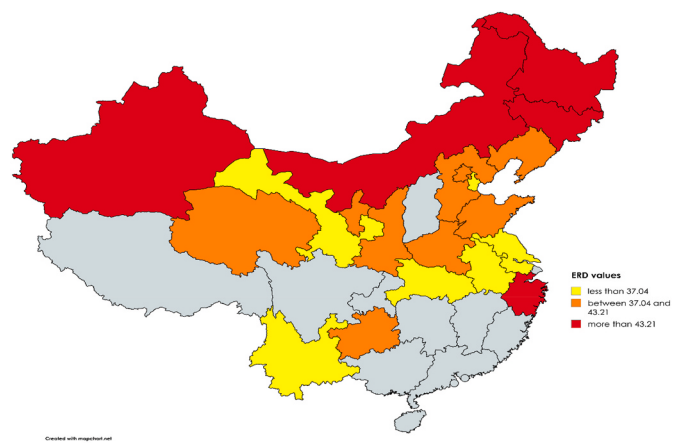
Frequency of valid observations (province–city–year combinations) in the final panel dataset.

Year	Province Frequency			City Frequency															
2008	127	Anhui	84	Aksu	12	Changzhou	4	Hami	12	Jining	12	Ningbo	8	Songyuan	12	Wuwei	12	Zhangjiakou	12
2009	127	Beijing	11	Altay	12	Chaoyang	12	Hangzhou	8	Jinzhou	12	Ordos	12	Southwest Guizhou Buyi and Miao Autonomous Prefecture	1	Wuzhong	12	Zhangye	12
2010	127	Gansu	97	Alxa League	12	Chengde	12	Hanzhong	12	Jiuquan	12	Pingliang	12	Suihua	12	Xiangyang	11	Zhaotong	3
2011	121	Guizhou	6	Ankang	12	Chifeng	12	Harbin	12	Jixi	12	Pu'er	3	Tacheng	12	Xianyang	12	Zhengzhou	12
2012	115	Hebei	84	Anqing	12	Chuxiong Yi Autonomous Prefecture	3	Hefei	12	Karamay	12	Qiandongnan Miao and Dong Autonomous Prefecture	1	Tai'an	12	Xilin Gol League	12	Zhongwei	12
2013	116	Heilongjiang	108	Anyang	12	Dali Bai Autonomous Prefecture	3	Heihe	12	Kashgar	12	Qiannan Buyi and Miao Autonomous Prefecture	1	Taizhou	8	Xingtai	12	Zhoukou	12
2014	116	Henan	84	Baishan	12	Dalian	12	Hohhot	12	Kizilsu Kirgiz Autonomous Prefecture	12	Qingdao	12	Tangshan	12	Xining	9	Zhoushan	8
2015	122	Hubei	88	Baoding	12	Dandong	12	Honghe Hani and Yi Autonomous Prefecture	3	Kunming	3	Qingyang	12	Tianjin	12	Xinyang	12	Zhumadian	12
2016	112	Inner Mongolia	132	Baoshan	3	Dehong Dai and Jingpo Autonomous Prefecture	3	Hotan	12	Lanzhou	1	Qinhuangdao	12	Tonghua	12	Xuzhou	4	Zibo	12
2017	129	Jiangsu	24	Baotou	12	Dingxi	12	Huanggang	11	Lianyungang	4	Qiqihar	12	Tongliao	12	Yan'an	12		
2018	129	Jilin	84	Bayannur	12	Diqing	3	Huangnan Tibetan Autonomous Prefecture	9	Liaocheng	12	Qujing	3	Tongren	1	Yanbian Korean Autonomous Prefecture	12		
2019	134	Liaoning	96	Bayingolin Mongolian Autonomous Prefecture	12	Enshi Tujia and Miao Autonomous Prefecture	11	Huangshan	12	Lijiang	3	Quzhou	8	Turpan	12	Yancheng	4		
Total	1475	Ningxia Qinghai	36 54	Beijing Bengbu	11 12	Fushun Fuxin	12	Hulunbuir	12	Lincang	3	Rizhao	12	Ulanqab	12	Yantai	12		
		Shaanxi	72	Bijie	1	Fuyang	12	Hung Yen League	12	Ili Kazakh Autonomous Prefecture	12	Longnan	12	Shaoxing	8	Weifang	12	Yichun	12
		Shandong	132	Binzhou	12	Gannan Tibetan Autonomous Prefecture	12	Jiamusi	12	Lu'an	12	Shenyang	12	Weihai	12	Yinchuan	12		
		Tianjin	12	Bortala Mongolian Autonomous Prefecture	12	Guiyang	1	Jilin	12	Mudanjiang	12	Shijiazhuang	12	Weinan	12	Yingkou	12		
		Xinjiang	168	Bozhou	12	Guoluo Tibetan	9	Jinan	12	Nanjing	4	Shiyan	11	Wenshan Miao Autonomous Prefecture	6	Yulin	12		

(continued on next page)

Table 3 (continued)

Year Frequency	Province Frequency	City Frequency	
			Autonomous Prefecture
			9 Jincheng
			11 Nantong
			4 Shuangyashan
			12 Wenzhou
			2 Yushu
			9 Tibetan Autonomous Prefecture
			3 Yuxi
Yunnan	45	Changchun	12 Halbei
			9 Jingmen
			11 Nantong
			4 Shuangyashan
			12 Wenzhou
			2 Yushu
			9 Tibetan Autonomous Prefecture
Zhejiang	58	Changi Hui Autonomous Prefecture	12 Haixi
			9 Jingzhou
			11 Nanyang
			12 Siping
			12 Wuhan
			11 Yuxi
			3 Yuxi
Total	1475		

**Fig. 2a.** Fig. 2 risk levels of LTD, HTD, ERD, and EED at the province level over the period 2008–2019.**Fig 2a** Medium values of LTD at the province level over the period 2008–2019.**Fig. 2b.** Medium values of HTD at the province level over the period 2008–2019.**Fig. 2c.** Medium values of ERD at the province level over the period 2008–2019.

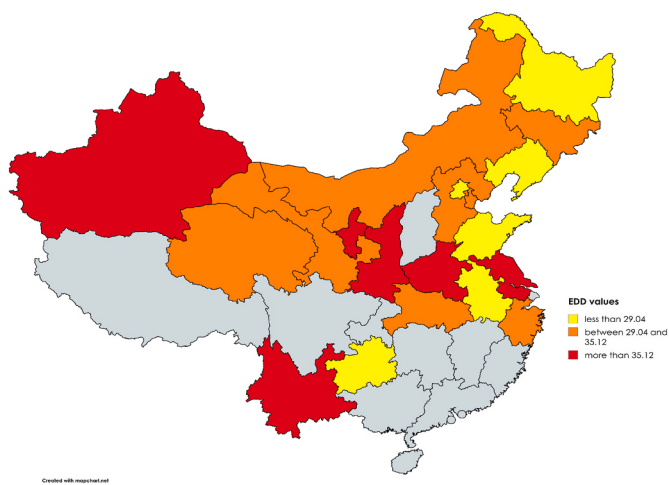


Fig. 2d. Medium values of EDD at the province level over the period 2008–2019.

Heilongjiang, Jiangsu, and Shaanxi (Qi and Wang, 2012; Gong et al., 2022; Zhang et al., 2022).

Now, as regards the trade-offs among these climate risk criteria, Table 4 reports on the results for the R matrix. The near-equal weights across the four climate risks suggest all phenomena contribute comparably to provincial climate vulnerability, reinforcing the need for integrated risk responses (Beillouin et al., 2020). For example, drought, rainfall, and temperature extremes all significantly impact agricultural productivity and water resource management, underscoring their equal relevance to policy planning (Beillouin et al., 2020; Wang and Liu, 2023).

The off diagonal, however, sheds more light into their intrinsic trade-offs. It is noticeable that extreme high temperatures and extreme rainfall present a negative trade-off of -0.969 (one index tends to increase to the detriment of the other). In regions experiencing prolonged heatwaves, the atmosphere may stabilize, suppressing convection and reducing the likelihood of rainfall (Miralles et al., 2019). This phenomenon is particularly evident in arid and semi-arid regions where heatwaves often coincide with dry spells. Conversely, areas with heavy rainfall are less likely to experience prolonged extreme heat due to the cooling effects of cloud cover and precipitation. For instance, in provinces such as Gansu or Ningxia, known for their arid climates, prolonged heat events may

further reduce rainfall, exacerbating drought conditions and water scarcity (Yang et al., 2015).

Nevertheless, extreme high temperatures are positively associated with extreme drought (6.202), followed by extreme low temperatures (3.803). High temperatures and drought often reinforce each other due to evapotranspiration feedbacks, especially during prolonged heatwaves. Provinces such as Qinghai and Yunnan, which are already experiencing rising high temperatures and drought, provide clear examples of this positive association (Gao et al., 2023). Besides, the increased variability in temperature extremes is a hallmark of climate change, where shifts in atmospheric circulation patterns lead to more pronounced swings between high and low extremes (Horton et al., 2015). In this sense, the destabilization of the jet stream, often attributed to Arctic warming, can result in extreme cold outbreaks during winter while also contributing to heatwaves in summer, which also happens in Qinghai and Yunnan.

The three remaining indexes (LTD, EDD, and ERD) tend to positively interact with one another, with a special note on the stronger interaction between extreme drought and extreme rainfall (3.982). It is well known that climate change increases the likelihood of hydrological extremes, where periods of severe drought are followed by intense rainfall events (Cawdry, 2023). Drought–flood alternations are linked to atmospheric moisture buildup and abrupt monsoon shifts in warming climates (Gao et al., 2023). This dynamic is observed in provinces like Yunnan, where the seasonal monsoon can lead to abrupt shifts between drought and heavy rainfall (Dong et al., 2023).

Finally, regions experiencing prolonged drought may also experience lower temperatures due to reduced vegetation cover and soil heat retention at night (Sungmin et al., 2022). Subsequent heavy rainfall can exacerbate cooling effects in such areas (Wouters et al., 2022). Additionally, disrupted precipitation patterns, such as those influenced by El Niño-Southern Oscillation (ENSO) events, can simultaneously trigger extremes in rainfall, drought, and temperature variability (Lv et al., 2022). Provinces such as Guizhou and Heilongjiang, characterized by significant climatic variability, may exemplify these interactions. For example, Guizhou's complex karst terrain and monsoonal climate contribute to frequent drought–flood alternations and overlapping extremes, including intensified droughts since the 1980s and increasing extreme rainfall events (Qin et al., 2021; Tan et al., 2024). Similarly, Heilongjiang has experienced sharp interannual swings in precipitation and a significant rise in temperature over the past century, with growing evidence of drought–flood alternation events linked to ENSO and Arctic teleconnections (Ma et al., 2025). These patterns illustrate how

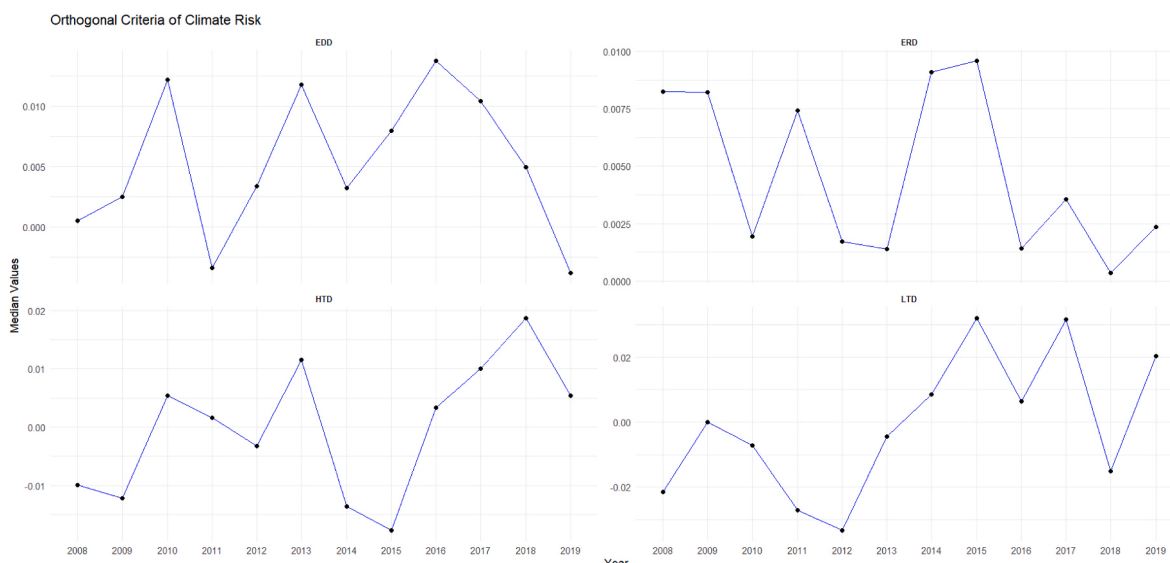


Fig. 3. Orthogonal climate risk criteria: evolution per year (median values).

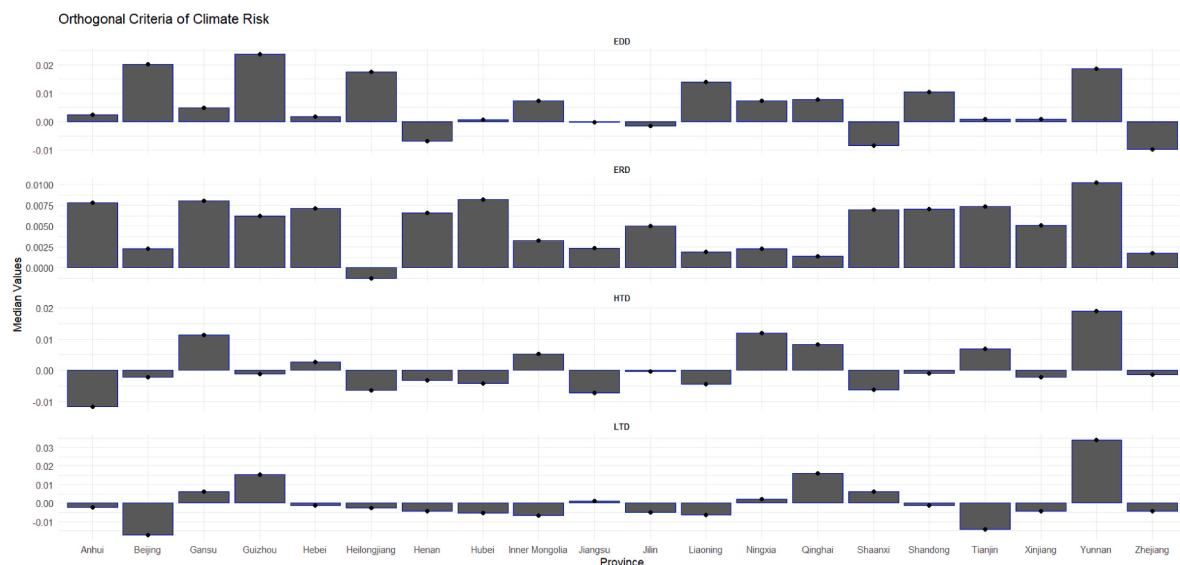


Fig. 4. Median values of the orthogonal (decorrelated) climate risk criteria (LTD, HTD, ERD, EDD) by province. These medians are computed over the entire study period (2008–2019).

Table 4
Trade-off matrix between climate risk criteria pairs. (*).

Trade-off	LTD	HTD	ERD	EDD
LTD	-38.393	3.803	0.594	1.212
HTD		38.204	-0.969	6.202
ERD		0.594	-0.969	3.982
EDD		1.212	6.202	-37.659

disrupted precipitation and temperature dynamics interact in provinces experiencing pronounced climate shifts.

Putting all these pieces together, these results suggest a transition in

the energy fuel matrix in the due course of the analyzed years (Wang et al., 2021), while sustaining growing economic activity and populational well-being. As regards this energy transition, Beijing, Shaanxi,

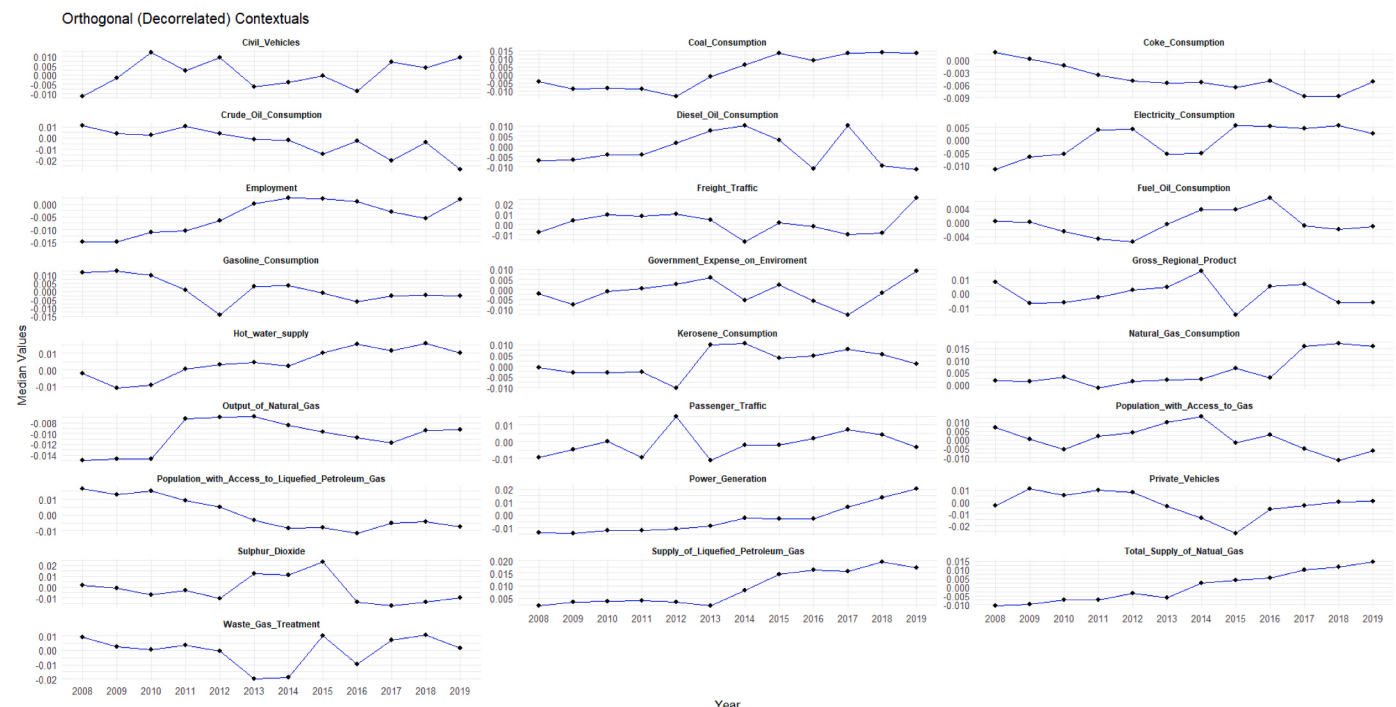


Fig. 5. Orthogonal contextual variables: evolution per year (median values).

and Xinjiang appear to be increasing their share on natural gas, while Yunnan still strongly relies on coal to sustain power generation (cf. Fig. 6), suggesting increased regional disparities (Zhao et al., 2022), where key areas are targeted to receive most investment in expanding infrastructure.

Besides, technological changes, beyond the energy matrix transition, appear to be the cause of a decrease in decorrelated levels of Sulfur dioxide emissions (cf. Fig. 5). The decline in decorrelated sulfur dioxide emissions reflects the adoption of desulfurization technologies in power plants and industrial facilities (Ding et al., 2019). These technologies, mandated by government regulations, have significantly reduced sulfur emissions despite continued reliance on coal in certain provinces (Liu et al., 2016). Technological upgrades in coal-fired power plants, such as ultra-supercritical steam cycle technology, also contribute to reduced emissions while maintaining high energy output (Tumanovskii et al., 2017). Nevertheless, strict enforcement of air pollution control measures, such as the Action Plan for Air Pollution Prevention and Control (2013–2017), played a pivotal role in reducing sulfur dioxide emissions by targeting key polluting industries.

With respect to the contextual variable relative weights and trade-offs (R matrix, cf. Table 5), the most important or discriminatory variables (with higher weights) among provinces and years are: employment, output of natural gas, power generation, supply of LPG, and hot water supply decorrelated levels (cf. main diagonal absolute values). On the other hand, the least discriminatory contextual variables are related to gross regional product, electricity consumption level, private vehicles, and civil vehicles.

As regards the trade-offs, where one variable increases to the detriment of the other, the most relevant are related to the following pairs: passenger traffic x supply of LPG, Sulfur dioxide x coal consumption, crude oil and fuel oil consumption x population with access to natural gas, government expenditure on environment x crude oil consumption, population with access to gas and supply of LPG x output of natural gas among others. Particularly, the trade-off between passenger traffic and LPG supply suggests competing priorities between expanding transportation networks and meeting household energy needs (Sovacool et al., 2023). Provinces with high LPG consumption may invest less in public transport infrastructure, reflecting differing development priorities (Collazos et al., 2024) (e.g., rural vs. urban focus). Similarly, there are competing uses for natural gas, where high output may favor industrial applications over expanding household access to gas or LPG

(Meidute-Kavaliauskienė et al., 2021). This dynamic is particularly relevant in resource-rich provinces prioritizing export or industrial usage.

On the other hand, most trade-ins are related to gross regional product, electricity consumption, and diverse types of fuel consumption x employment levels. Trade-ins (positive associations) suggest variables that reinforce one another, often driven by complementary relationships or synergistic effects. For example, electricity consumption supports industrial activity, which in turn drives employment (Kouakou, 2011). Provinces with high employment levels often exhibit higher electricity usage, reflecting energy-intensive industries (Narayan and Smyth, 2005). Additionally, fuel consumption (e.g., crude oil, diesel) is closely linked to employment in sectors such as manufacturing, logistics, and transportation, where energy serves as a key input for production.

Results for the unweighted trade-offs among climate criteria risk and contextual variables allow a segmented analysis on the critical drivers relating to each climate hazard (cf. Fig. 7, on the left). It is noteworthy to have the impact of power generation and coal consumption on the increase of lower extreme temperatures. Coal-fired power plants are significant contributors to localized air pollution, including particulates that can modify atmospheric radiation and cooling, potentially exacerbating extreme low-temperature events (Guttikunda and Jawahar, 2014). Increased energy demand during colder periods may lead to higher coal consumption, further reinforcing this relationship (Kim and Lee, 2019). Provinces with high coal dependency (e.g., Shanxi, Inner Mongolia) may experience such effects due to the combined impacts of emissions and cooling from heavy air pollution during winter months.

Also noticeable is the impact of economic activity (gross regional product), Sulfur dioxide emissions, and population with access to LPG on the increase of extreme rainfall. High levels of economic activity often involve increased energy consumption, urbanization, and industrial emissions, all of which can influence local and regional climate systems (Li and Lin, 2015). Urban heat islands can enhance convection and precipitation, leading to extreme rainfall events (Zhong et al., 2015). Besides, Sulfur dioxide is a precursor to aerosols that modify cloud microphysics, increasing the likelihood of intense precipitation under certain conditions (Lin et al., 2018). Lastly, increased LPG access may correlate with urbanization and infrastructure expansion, both of which are associated with higher surface runoff and localized flooding risks during rainfall events. Eastern provinces such as Jiangsu and Zhejiang, which have high GRP and urbanization levels, frequently

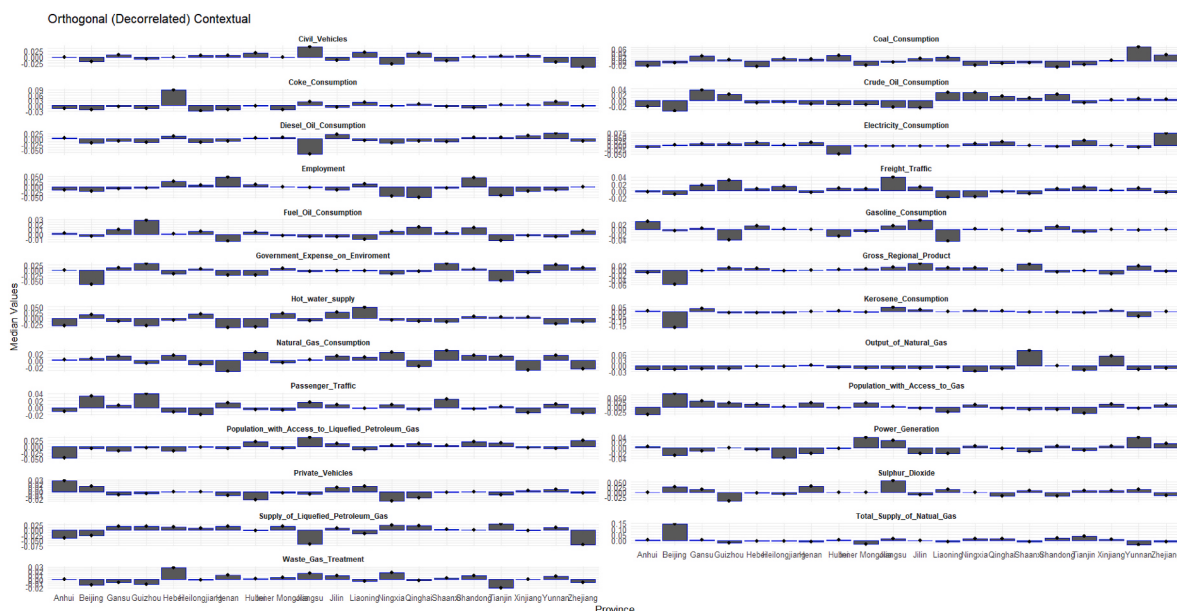


Fig. 6. Orthogonal contextual variables: median values per province.

Table 5

Trade-off matrix between contextual variable pairs. (*).

Contextual Trade-offs	Employment	Output_of_Natural_Gas	Power_Generation	Total_Supply_of_Natural_Gas	Population_with_Access_to_Gas	Supply_of_Liquefied_Petroleum_Gas	Hot_water_supply	Coal_Consumption	Coke_Consumption	Crude_Oil_Consumption	Kerosene_Consumption	Diesel_Oil_Consumption	Fuel_Oil_Consumption	Natural_Gas_Consumption	Electricity_Consumption	Sulphur_Dioxide	Govern_Expense_on_Environment	Civil_Vehicles	Private_Vehicles	Passenger_Traffic	Freight_Traffic	Waste_Gas_Treatment	Gross_Regional_Product		
Employment	38.39	-11.39	21.14	14.88	28.24	13.27	19.63	13.30	26.11	21.66	19.65	26.08	8.04	27.39	19.50	18.81	26.76	16.00	20.14	27.02	26.38	16.67	23.25	22.16	27.55
Output_of_Natural_Gas	0.00	36.66	1.44	11.12	2.57	-11.54	11.93	4.47	3.65	-1.79	5.00	-4.40	1.55	-0.30	-0.39	22.71	1.83	0.41	-1.68	0.20	0.16	-1.13	3.66	1.53	-1.10
Power_Generation	0.00	0.00	32.02	15.16	10.40	-0.20	-1.90	-0.74	19.90	4.59	5.18	9.08	7.06	10.05	10.98	14.18	23.29	-0.12	2.71	15.54	15.91	-1.52	15.89	13.37	14.82
Total_Supply_of_Natural_Gas	0.00	0.00	0.00	29.99	19.20	4.18	-2.73	4.91	-4.58	2.05	11.17	8.20	20.08	2.39	10.37	19.80	8.17	1.96	31.62	14.70	14.52	0.54	1.94	5.88	15.27
Population_with_Access_to	0.00	0.00	0.00	0.00	-13.91	-7.70	0.15	1.12	2.47	-1.18	14.65	10.84	5.89	-9.01	13.08	0.09	-2.32	6.56	4.20	10.48	-10.51	-2.42	3.22	-5.19	-10.57
Supply_of_Liquefied_Petrol	0.00	0.00	0.00	0.00	0.00	-32.98	25.69	4.83	0.60	2.46	-6.62	12.66	-4.47	2.17	0.95	1.55	-4.25	-8.87	0.34	2.95	3.36	22.03	9.09	4.31	-5.21
Population_with_Access_to	0.00	0.00	0.00	0.00	0.00	0.00	16.59	7.32	0.46	-4.74	1.86	4.40	1.67	6.92	8.46	-1.81	1.83	8.73	3.67	-0.33	-1.55	6.60	7.37	4.18	4.41
Hot_water_supply	0.00	0.00	0.00	0.00	0.00	0.00	34.27	8.43	4.06	15.51	2.31	1.03	4.36	6.73	3.83	1.27	2.04	-1.29	-0.71	-0.56	-1.47	5.32	3.46	-6.25	
Coal_Consumption	0.00	0.00	0.00	0.00	0.00	0.00	0.00	16.85	11.28	3.08	6.77	13.44	2.12	-2.32	1.34	-2.53	9.56	3.47	3.61	3.85	5.77	-0.34	-6.70	2.30	
Coke_Consumption	0.00	0.00	0.00	0.00	0.00	0.00	0.00	0.00	28.33	0.86	0.84	-4.86	1.43	-3.97	4.21	5.97	4.39	7.22	5.74	5.81	-0.05	0.36	2.34	1.28	
Crude_Oil_Consumption	0.00	0.00	0.00	0.00	0.00	0.00	0.00	0.00	0.00	19.97	-3.32	-5.96	6.68	13.34	-0.71	3.28	8.95	-3.22	-0.36	-1.95	0.63	2.52	3.60	-1.51	
Gasoline_Consumption	0.00	0.00	0.00	0.00	0.00	0.00	0.00	0.00	0.00	16.28	-2.75	0.52	7.01	-1.86	1.53	4.05	-0.56	1.92	2.09	-1.35	4.11	5.24	-0.99		
Kerosene_Consumption	0.00	0.00	0.00	0.00	0.00	0.00	0.00	0.00	0.00	0.00	25.46	-0.12	-2.38	3.55	2.20	-0.90	2.36	-0.95	-1.18	-1.01	0.09	2.03	0.05		
Diesel_Oil_Consumption	0.00	0.00	0.00	0.00	0.00	0.00	0.00	0.00	0.00	0.00	0.00	2.61	4.40	-0.96	-0.70	8.60	2.19	0.26	0.23	3.08	3.49	0.64	-0.46		
Fuel_Oil_Consumption	0.00	0.00	0.00	0.00	0.00	0.00	0.00	0.00	0.00	0.00	0.00	0.00	16.60	-4.12	0.68	0.36	-0.70	0.12	0.37	-1.63	1.65	9.35	-0.11		
Natural_Gas_Consumption	0.00	0.00	0.00	0.00	0.00	0.00	0.00	0.00	0.00	0.00	0.00	0.00	0.00	14.60	-3.48	-3.07	-0.68	-2.70	2.31	0.18	1.14	-2.12	-1.92		
Electricity_Consumption	0.00	0.00	0.00	0.00	0.00	0.00	0.00	0.00	0.00	0.00	0.00	0.00	0.00	0.00	0.00	0.00	0.00	0.00	0.00	0.00	14.59	2.90	-0.05		
Sulphur_Dioxide	0.00	0.00	0.00	0.00	0.00	0.00	0.00	0.00	0.00	0.00	0.00	0.00	0.00	0.00	0.00	0.00	0.00	0.00	0.00	0.00	0.00	0.00	3.60		
Government_Expense...	0.00	0.00	0.00	0.00	0.00	0.00	0.00	0.00	0.00	0.00	0.00	0.00	0.00	0.00	0.00	0.00	0.00	0.00	0.00	0.00	0.00	0.00	6.76		
Civil_Vehicles	0.00	0.00	0.00	0.00	0.00	0.00	0.00	0.00	0.00	0.00	0.00	0.00	0.00	0.00	0.00	0.00	0.00	0.00	0.00	0.00	0.00	0.00	1.83		
Private_Vehicles	0.00	0.00	0.00	0.00	0.00	0.00	0.00	0.00	0.00	0.00	0.00	0.00	0.00	0.00	0.00	0.00	0.00	0.00	0.00	0.00	0.00	0.00	-1.31		
Passenger_Traffic	0.00	0.00	0.00	0.00	0.00	0.00	0.00	0.00	0.00	0.00	0.00	0.00	0.00	0.00	0.00	0.00	0.00	0.00	0.00	0.00	0.00	0.00	0.90		
Freight_Traffic	0.00	0.00	0.00	0.00	0.00	0.00	0.00	0.00	0.00	0.00	0.00	0.00	0.00	0.00	0.00	0.00	0.00	0.00	0.00	0.00	0.00	0.00	0.14		
Waste_Gas_Treatment	0.00	0.00	0.00	0.00	0.00	0.00	0.00	0.00	0.00	0.00	0.00	0.00	0.00	0.00	0.00	0.00	0.00	0.00	0.00	0.00	0.00	0.00	-18.01		
Gross_Regional_Product	0.00	0.00	0.00	0.00	0.00	0.00	0.00	0.00	0.00	0.00	0.00	0.00	0.00	0.00	0.00	0.00	0.00	0.00	0.00	0.00	0.00	0.00	5.03		

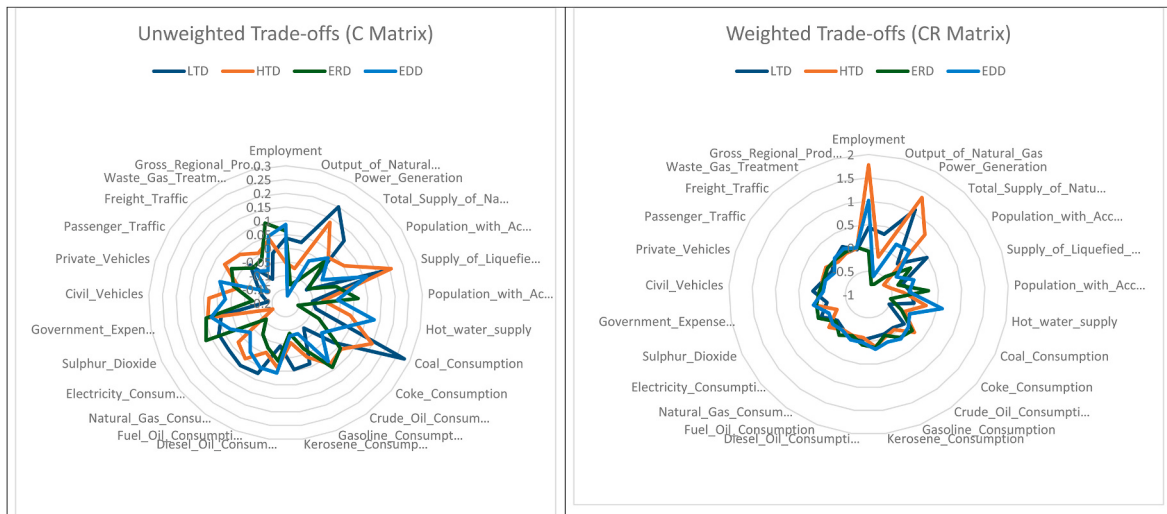


Fig. 7. Unweighted (C matrix) and weighted (CR matrix) trade-off coefficients among climate risk criteria and contextual variables. (*) (**). (*) Unweighted trade-offs are also equivalent to the coefficients of the decorrelated contextual variables (IVs) obtained from the four OLS regressions performed separately for each decorrelated climate criteria risk (DVs). (**) Weighted trade-offs are obtained from the multiplication of three matrices: one related to the contextual variable trade-offs (Table 5), the other, to the unweighted trade-offs here presented, and the last, to the climate criteria trade-offs (Table 4).

experience extreme rainfall events influenced by such factors (Shen et al., 2022).

On the other hand, passenger traffic, private vehicles, and civil vehicles appear to be key drivers to explain the increase of extreme high temperatures. Transportation contributes significantly to greenhouse gas emissions, particularly carbon dioxide, which amplifies the greenhouse effect and contributes to temperature increases (Ramanathan and Feng, 2009). Urban areas with high vehicle density are especially prone to the urban heat island effect, where heat is retained by asphalt, concrete, and reduced vegetation cover (Kolbe, 2019). High-density urban centers such as Beijing and Shanghai, with heavy passenger and private vehicle traffic, often experience extreme high-temperature events driven

by these factors.

Finally, extreme drought seems to be related to higher levels of employment, fuel oil, and diesel oil consumption, besides hot water supply and private vehicles (Perera, 2018). High employment levels are often associated with energy-intensive industries, which can increase water demand and exacerbate drought conditions (Ma et al., 2024). For instance, thermoelectric power plants require significant water for cooling, contributing to local water scarcity (Pan et al., 2018). Additionally, diesel and fuel oil usage is linked to agricultural and industrial activities, which are major water consumers. Excessive water withdrawals for these purposes can intensify drought severity (Pedro-Monzonís et al., 2015). Similarly, regions with high hot water

supply levels likely have significant energy demands that further strain water resources (Li et al., 2015). Lastly, vehicle use, while less directly linked, may contribute to drought indirectly through emissions and urbanization, which alter local hydrological cycles (Huang et al., 2024). Provinces such as Yunnan and Guizhou, with significant agricultural and industrial activities, exemplify these relationships (Yang et al., 2022).

However, while all these climate risk issues are interconnected to some extent, it is deemed necessary to bound these coefficients with respect to the contextual variables and climate criteria risk trade-offs (cf. Fig. 7, on the right). Consistent with previous work, our CCDTW framework confirms that employment, power generation, and natural-gas access are the top drivers of provincial climate risk (Wu and Lin, 2022; Zhao and Wang, 2015); below we focus on what new insights the weighting reveals. Then, the common critical climate drivers emerge: employment, power generation, and population with access to natural gas. Putting in other words, how to sustain economic welfare with minimal climate jeopardy generated by energy production learning lessons from each other.

The normalized CRI (Climate Risk Index) can be computed by the summation of the CR matrix coefficients for each observation, thus allowing the rank and benchmark across Chinese provinces over the years. As a benchmark, the normalized CRI enables standardized comparisons of climate risk both across space (between provinces) and over time. It allows for the identification of consistently high-risk provinces, as well as those showing improvement, providing a valuable tool for regional prioritization. Policymakers can use the CRI to classify provinces into relative risk categories—high, medium, or low—thereby informing strategic planning, resource allocation, and adaptation efforts. To categorize provinces into high, moderate, and low climate risk groups, we used the distribution of the normalized Climate Risk Index (CRI) scores across all observations. Specifically, we classified: (i) provinces with CRI values in the top 25th percentile as high-risk, (ii) those between the 25th and 75th percentile as moderate-risk, and (iii) those in the bottom 25th percentile as low-risk. This percentile-based classification provides a transparent and interpretable framework to rank and compare provinces relative to each other over time. The thresholds are not based on absolute hazard levels, but on relative climate vulnerability as measured by the CCDTW-derived CRI, making the classification useful for intra-national benchmarking and policy prioritization. For instance, provinces with persistently high CRI scores despite socio-economic growth may need targeted environmental interventions, while those with declining CRI values can serve as reference cases or models for others. This benchmarking capacity is illustrated in Fig. 8 and Table 6, which capture the distribution and rank ordering of provincial risk levels. Fig. 8 shows that the CRI distribution is skewed to the left, suggesting most provinces experienced low to moderate climate risk during the study period. However, interprovincial differences remain substantial. Table 6 presents the OLS regression results of CRI against year and province, highlighting significant time trends and regional variation. Using Anhui as the reference, the model reveals that provinces like Jilin and Guizhou do not differ significantly in risk, while

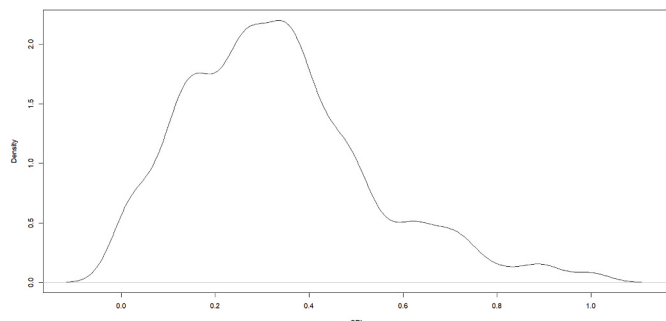


Fig. 8. Density plot for the CRI.

Table 6

OLS for the CRI decomposition across Chinese provinces over time.

Terms	Estimate	Std. Error	t value	Pr(> t)
(Intercept)	-47.2179	0.9067	-52.0782	0.0000
Year	0.0236	0.0005	52.3139	0.0000
Province Beijing	0.1283	0.0188	6.8182	0.0000
Province Gansu	0.0330	0.0087	3.7664	0.0002
Province Guizhou	0.0404	0.0248	1.6270	0.1040
Province Hebei	0.3677	0.0091	40.5950	0.0000
Province Heilongjiang	0.1116	0.0085	13.0719	0.0000
Province Henan	0.3740	0.0091	41.2913	0.0000
Province Hubei	0.1696	0.0090	18.9422	0.0000
Province Inner Mongolia	0.1980	0.0082	24.1651	0.0000
Province Jiangsu	0.1802	0.0136	13.2368	0.0000
Province Jilin	0.0021	0.0091	0.2362	0.8133
Province Liaoning	0.1394	0.0088	15.8939	0.0000
Province Ningxia	-0.1009	0.0117	-8.6288	0.0000
Province Qinghai	-0.1895	0.0102	-18.5126	0.0000
Province Shaanxi	-0.0418	0.0094	-4.4346	0.0000
Province Shandong	0.4390	0.0082	53.5895	0.0000
Province Tianjin	-0.0919	0.0181	-5.0758	0.0000
Province Xinjiang	-0.0719	0.0078	-9.1657	0.0000
Province Yunnan	0.1107	0.0110	10.0396	0.0000
Province Zhejiang	0.0771	0.0101	7.6656	0.0000

Residual standard error: 0.0587 on 1454 degrees of freedom Multiple R-squared: 0.9149, Adjusted R-squared: 0.9137 F-statistic: 781.5 on 20 and 1454 DF, p-value: <2.2e-16.

P values below 0.05 in bold.

others deviate strongly—supporting the CRI's discriminatory power as a benchmarking tool.

However, the remainder provinces present a very heterogeneous scenario. Shaanxi, Xinjiang, Tianjin, Ningxia, and Qinghai below the mean CRI values, whose best environmental practices should be learnt and spread across the other provinces. These provinces may have implemented effective mitigation strategies, such as transitioning to cleaner energy sources, adopting advanced industrial technologies, or enforcing stricter environmental regulations (Jiang and Reza, 2024). For example: Xinjiang and Qinghai executed significant investments in renewable energy, including solar and wind power, which are likely contributed to reduced climate risks (Harlan, 2023). In turn, urban environmental management and industrial optimization efforts in Tianjin may have reduced its CRI (Feng et al., 2019). On the other hand, provinces like Ningxia and Shaanxi, located in drier regions, might naturally experience fewer climate hazards like extreme rainfall or flooding, contributing to their lower CRI values (Dai et al., 2009).

In an opposite direction, Shandong, Henan, Hebei, Inner Mongolia, Jiangsu, Hubei, and Liaoing lead the provinces, in order, with higher climate risk index and merit attention. These provinces are highly industrialized and densely populated, leading to greater emissions, land-use changes, and energy demands. For example, Shandong is a major industrial hub, with significant coal consumption and emissions (Jing et al., 2021); Jiangsu and Henan exhibit high levels of urbanization and industrialization that could contribute to increased climate vulnerabilities (Hou et al., 2022). In a different way, however, provinces in the North China Plain, like Hebei and Henan, are prone to extreme weather events such as heatwaves and droughts, exacerbating their CRI values (Zhao et al., 2024). And there is the particular case of Inner Mongolia's reliance on coal and heavy industry, which increases its climate risk, despite efforts to transition to renewables (Guan et al., 2024).

Also noteworthy is the situation of Beijing, altogether with Heilongjiang and Yunnan in an intermediate ranking position. Despite being a highly urbanized and industrialized region, Beijing's aggressive environmental policies, such as switching to natural gas and reducing coal use, likely mitigate its CRI, placing it in the intermediate range (Lewis and Edwards, 2021). Heilongjiang, a northeastern province, with a strong agricultural base, exhibits moderate risks driven by vulnerabilities to extreme temperatures and rainfall but benefits from less

industrial activity compared to higher-risk provinces (Zhang et al., 2024). At last, Yunnan's reliance on coal for power generation contributes to moderate climate risks, but its significant renewable energy development (e.g., hydropower) may help offset some vulnerabilities (Peng et al., 2023).

5. Comparative advantages and novel insights of the CCDTW framework

The CCDTW (Criteria and Context Decomposition for Trade-Off Weighting) framework offers distinct methodological and analytical advantages over traditional approaches to climate risk assessment such as PCA-weighted indices, entropy-based MCDM, or regression-only models. These advantages are fourfold. First, CCDTW addresses the issue of multicollinearity by applying QR decomposition to both the climate risk criteria and the contextual variable matrices. This process orthogonalizes the input variables, meaning it transforms them into statistically independent dimensions without altering their span. In contrast, many conventional approaches either ignore multicollinearity (leading to inflated or unstable weights) or address it using methods like PCA, which often result in composite latent variables that obscure the interpretability of individual indicators.

Second, the CCDTW approach preserves the interpretability of original variables, even after decorrelation. Unlike PCA, where original variables are replaced by abstract components, QR decomposition allows the reconstruction of variable-level importance and interaction patterns through the resulting triangular matrix R . This makes it possible to identify which original criteria or contextual factors are most influential, and how they interact with others.

Third, CCDTW explicitly quantifies trade-offs among variables using the off-diagonal elements of the R matrices. These elements capture the degree to which one variable contributes to or substitutes for another in the presence of correlation. This capability is largely absent from traditional MCDM methods, which typically treat all variables as additive and independent in their contribution to the overall score.

Fourth, CCDTW introduces a context-sensitive integration of climate risk criteria with socio-economic variables. Rather than building an index solely from environmental indicators, CCDTW uses a structured regression framework to model how contextual drivers (e.g., employment, energy use) influence each dimension of climate risk. This enables a more nuanced understanding of risk exposure and vulnerability that accounts for local conditions.

Finally, the construction of the Climate Risk Index (CRI) in CCDTW is based on weighted trade-off coefficients that combine the structure of both the criteria and contextual matrices. These weights are not arbitrarily assigned or derived solely from data variability (as in entropy weighting), but rather emerge from a three-part interaction: the independent effects of contextual variables, the importance and correlation structure of criteria, and the interaction patterns between both. This results in a more balanced and empirically grounded index that is robust, interpretable, and policy-relevant.

Because the CCDTW framework combines orthogonalization, trade-off structure, and contextual regression, it enabled us to derive insights that would not have been possible with simpler methods, including tht.

- Isolation of critical drivers, by analyzing the weighted CR matrix, we identified employment, power generation, and population access to natural gas as the top contextual contributors to climate risk — even after adjusting for their interdependence and overlap. Traditional regression or PCA would either mask these overlaps or overstate their effects due to multicollinearity.
- Quantified inter-variable trade-offs, for example, the CCDTW revealed a strong negative trade-off (-0.969) between extreme rainfall and extreme heat (from the R matrix), suggesting physical-climatic substitution patterns that standard scoring models ignore.

- Region-specific risk signatures, where the decorrelated structure allowed us to map unique climate-context patterns at the provincial level (e.g., drought/heat interaction in Ningxia vs. urban-heat-emissions link in Jiangsu), which would have been blurred in PCA or entropy-MCDM models.

- Balanced treatment of criteria since, unlike entropy methods that may overweight rare variables (e.g., ERD), the CCDTW treated all criteria equally at first, then allowed weighting to emerge from structure and interaction — improving fairness and traceability.

So, while CCDTW involves additional steps (QR decomposition, multiple matrix multiplications), it is computationally tractable even for medium-to-large datasets like this study with almost 1500 observations.

6. Conclusions

The increasing impacts of climate change on socio-economic and environmental systems necessitate advanced methodologies for assessing and mitigating risks. This paper introduced the Criteria and Context Decomposition for Trade-Off Weighting (CCDTW) framework, a novel multi-criteria decision-making (MCDM) approach designed to address these challenges at the provincial level in China. By integrating QR decomposition and weighted trade-offs, the CCDTW framework offers a robust mechanism to decorrelate risk criteria, quantify trade-offs, and construct a Climate Risk Index (CRI) that ranks and benchmarks provinces over time.

Climate change poses multifaceted risks that vary across regions and sectors, making adaptive and region-specific responses essential for mitigating its adverse effects. This study contributes to this effort by advancing climate risk assessment methodologies and providing actionable insights for decision-makers in one of the world's most climate-vulnerable nations. The CCDTW framework addresses the limitations of traditional risk assessment methods by accounting for socio-economic contexts and interactions among climate criteria, offering a more comprehensive and dynamic tool for policy and planning.

This paper makes several important contributions. Methodologically, the CCDTW framework combines QR decomposition with trade-off weighting, enabling a detailed analysis of interdependencies among climate risk criteria and socio-economic variables. Practically, the development of the CRI facilitates the ranking of Chinese provinces, providing policymakers with region-specific climate risk profiles and trends. Furthermore, by incorporating socio-economic drivers such as employment, energy use, and population access to resources, the CCDTW offers a holistic understanding of climate risk dynamics. Additionally, the framework highlights significant temporal trends and spatial disparities in climate risks across Chinese provinces, offering insights for both immediate and long-term interventions.

The application of the CCDTW framework to a non-balanced panel dataset of 1457 observations revealed several significant findings. Provinces such as Shandong, Henan, and Hebei exhibit the highest climate risk, driven by high industrial activity and energy consumption. Temporal trends indicate increasing risks associated with extreme temperatures and rainfall, reflecting the broader impacts of global climate change. Socio-economic variables, including employment and power generation, are key drivers of climate risk, underscoring the trade-offs between economic development and climate mitigation. On the other hand, provinces like Shaanxi and Qinghai demonstrate lower climate risks, showcasing best practices in climate adaptation and energy transition.

The results of this study have important policy implications: 1) High-risk provinces (e.g., Shandong, Henan, Hebei) should prioritize stringent emission reduction policies, improve renewable energy adoption, and enhance climate resilience planning; 2) Moderate-risk provinces (e.g., Beijing, Yunnan, Heilongjiang) should leverage technological advancements to further mitigate climate risk while maintaining economic stability; 3) Low-risk provinces (e.g., Shaanxi, Qinghai) serve as models for

best practices in climate adaptation and energy efficiency, which could be scaled to high-risk areas; 4) Policymakers should consider setting a CRI threshold above which climate mitigation measures become mandatory, ensuring targeted interventions in the most vulnerable regions.

While the CCDTW framework offers significant advancements, certain limitations remain. The analysis relies on available datasets, which may not capture all relevant variables or reflect real-time changes. Expanding data sources and incorporating high-resolution datasets could enhance future applications. Additionally, the QR decomposition and weighting process, while robust, may require further simplification to improve usability for non-technical stakeholders. Although applied to Chinese provinces, the framework could be extended to other regions or scaled for global comparisons. Future research could explore its adaptability to diverse geographic and socio-economic contexts.

In conclusion, the CCDTW framework represents a significant step forward in climate risk assessment, offering a powerful tool for

identifying vulnerabilities and informing targeted climate adaptation strategies. By integrating methodological innovation with practical application, this study provides a foundation for advancing climate resilience in China and beyond.

CRediT authorship contribution statement

Peter Wanke: Writing – original draft, Visualization, Software, Formal analysis, Conceptualization. **Yong Tan:** Writing – review & editing, Writing – original draft, Formal analysis, Data curation, Conceptualization.

Declaration of competing interest

The authors declare that they have no known competing financial interests or personal relationships that could have appeared to influence the work reported in this paper.

Appendix A. The names and locations of Chinese provinces in the map



Appendix B

Medium values of LTD, HTD, ERD and EDD at the province level over the period 2008–2019

	Provinces	LTD	HTD	ERD	EDD
1	Anhui	47.24	52.44	34.92	26.94
2	Beijing	54.29	61.81	38.89	18.99
3	Gansu	43.05	69.83	32.41	32.54
4	Guizhou	43.14	60.31	43.21	22.29
5	Hebei	50.11	59.37	41.67	29.69
6	Heilongjiang	51.20	59.07	58.06	19.68
7	Henan	52.44	57.98	40.28	40.82
8	Hubei	47.98	56.18	29.63	33.76
9	Inner Mongolia	52.55	60.68	48.69	29.04
10	Jiangsu	43.71	54.17	36.51	39.15
11	Jilin	47.53	60.54	50.62	33.83
12	Liaoning	51.55	58.96	37.04	26.30

(continued on next page)

Appendix B (continued)

	Provinces	LTD	HTD	ERD	EDD
13	Ningxia	45.52	70.37	38.89	40.51
14	Qinghai	33.93	67.25	43.06	34.02
15	Shaanxi	42.64	53.85	41.67	43.99
16	Shandong	47.37	58.66	41.67	25.11
17	Tianjin	57.58	66.09	33.33	34.18
18	Xinjiang	45.45	58.61	48.77	43.23
19	Yunnan	29.39	81.98	33.59	36.31
20	Zhejiang	44.40	62.44	48.61	35.21

Data availability

Data will be made available on request.

References

- Andrista, S., Utami, N.P., Hukom, V., Nielsen, M., Neilsen, R., 2025. Responses to climate change: perceptions and adaptation among small-scale farmers in Indonesia. *J. Environ. Manag.* 377, 124593.
- Attflö, L.A., 2025. Spillover effects of climate policy uncertainty on green innovation. *J. Environ. Manag.* 375, 1243334.
- Bellouin, D., Schaubiger, B., Bastos, A., Caias, P., Makowski, D., 2020. Impact of extreme weather conditions on European crop production in 2018. *Philos. Trans. R. Soc. B* 375 (1810), 20190510.
- Bevacqua, E., Schleussner, C.F., Zscheischler, J., 2025. A year above 1.5 °C signals that Earth is most probably in the 20-year period that will reach the Paris Agreement limit. *Nat. Clim. Change* 15, 262–265.
- Cawdrey, K., 2023. Warming Makes Droughts, Extreme Wet Events More Frequent, Intense. NASA.
- Collazos, J.S.G., Ardila, L.M.C., Cardona, C.J.F., 2024. Energy transition in sustainable transport: concepts, policies, and methodologies. *Environ. Sci. Pollut. Control Ser.* 31, 58669–58686.
- Dai, J., Ge, Q., Xiao, S., Wang, M., Wu, W., Cui, H., 2009. Wet-dry changes in the borderland of Shaanxi, Gansu and Ningxia from 1208 to 1369 based on historical records. *J. Geogr. Sci.* 19, 750–764.
- Dawson, R.J., 2015. Handling interdependencies in climate change risk assessment. *Climate* 3, 1079–1096.
- Ding, X., Li, Q., Wu, D., Liang, Y., Xu, X., Xie, G., Wei, Y., Sun, H., Zhu, C., Fu, H., Chen, J., 2019. Unexpectedly increased particle emissions from the steel industry determined by Wet/Semidry/Dry flue gas desulfurization technologies. *Environ. Sci. Technol.* 53, 10361–10370.
- Dong, Z., Gui, S., Yang, R., Cheng, J., Yang, H., Ma, J., 2023. Interdecadal variation of precipitation over Yunnan, China in summer and its possible causes. *Front. Environ. Sci.* 11, 1281202.
- Ebi, K.L., Kovats, R.S., Menne, B., 2006. An approach for assessing human health vulnerability and public health interventions to adapt to climate change. *Environ. Health Perspect.* 114, 1930–1934.
- Esperón-Rodríguez, M., Bonifacio-Bautista, M., Barradas, V.L., 2016. Socio-economic vulnerability to climate change in the central mountainous region of eastern Mexico. *Ambio* 45, 146–160.
- Feng, D., Li, J., Li, X., Zhang, Z., 2019. The effects of urban sprawl and industrial agglomeration on environmental efficiency: evidence from the Beijing-Tianjin-Hebei urban agglomeration. *Sustainability* 11, 3042.
- Gao, L., Han, X., Chen, X., Liu, B., Li, Y., 2023. The spring drought in Yunnan Province of China: variation characteristics, leading impact factors, and physical mechanisms. *Atmosphere* 14, 294.
- Goessling, H.F., Rackow, T., Jung, T., 2025. Recent global temperature surge intensified by record-low planetary albedo. *Science* 387 (6729), 68–73.
- Gong, X., Wang, X., Li, Y., Ma, L., Li, M., Si, H., 2022. Observed changes in extreme temperature and precipitation indices on the Qinghai-Tibet Plateau, 1960–2016. *Front. Environ. Sci.* 10, 888937.
- Gu, M., Eisenstat, S.C., 1996. Efficient algorithms for computing a strong rank-revealing QR factorization. *SIAM J. Sci. Comput.* 17, 848–869.
- Gu, L., Yin, J., Gentine, P., Wang, H.-M., Salter, L.J., Sullivan, S.C., Chen, J., Zscheischler, J., Guo, S., 2023. Large anomalies in future extreme precipitation sensitivity driven by atmospheric dynamics. *Nat. Commun.* 14, 3197.
- Guan, X.-g., Ren, F.-r., Fan, G., Zhang, Q.-q., Wu, T.-f., 2024. Dynamic evaluation and sensitivity analysis of China's industrial solid waste management efficiency based on ecological environment cycle perspective. *Front. Environ. Sci.* 12, 1462975.
- Guttikunda, S.K., Jawahar, P., 2014. Atmospheric emissions and pollution from the coal-fired thermal power plants in India. *Atmos. Environ.* 92, 449–460.
- Harlan, T., 2023. Low-carbon frontier: renewable energy and the new resource boom in Western China. *China Q.* 255, 591–610.
- Horton, D., Johnson, N.C., Singh, D., Swain, D.L., Rajaratnam, B., Diffenbaugh, N.S., 2015. Contribution of changes in atmospheric circulation patterns to extreme temperature trends. *Nature* 522, 465–469.
- Hou, W., Wu, S., Yang, L., Yin, Y., Gao, J., Deng, H., Wu, M., Li, X., Liu, L., 2022. Production-living-ecological risk assessment and corresponding strategies in China's provinces under climate change scenario. *Land* 11, 1424.
- Huang, S., Wang, S., Gan, Y., Wang, C., Horton, D.E., Li, C., Zhang, X., Niyogi, D., Xia, J., Chen, N., 2024. Widespread global exacerbation of extreme drought induced by urbanization. *Nature Cities* 1, 597–609.
- Jiang, B., Reza, M.Y., 2024. Renewable energy for sustainable development in China: discourse analysis. *PLoS One* 19, e0298347.
- Jing, X., Tian, G., Li, M., Javeed, S.A., 2021. Research on the spatial and temporal differences of China's provincial carbon emissions and ecological compensation based on land carbon budget accounting. *Int. J. Environ. Res. Publ. Health* 18, 12892.
- Kim, Y., Lee, S., 2019. Trends of extreme cold events in the central regions of Korea and their influence on the heating energy demand. *Weather Clim. Extrem.* 24, 100199.
- Kolbe, K., 2019. Mitigating urban heat island effect and carbon dioxide emissions through different mobility concepts: Comparison of conventional vehicles with electric vehicles, hydrogen vehicles and public transportation. *Transp. Policy* 80, 1–11.
- Kouakou, A.K., 2011. Economic growth and electricity consumption in Côte d'Ivoire: evidence from time series analysis. *Energy Policy* 39, 3638–3644.
- Lewis, J., Edwards, 2021. Assessing China's Energy and Climate Goals. the Centre for American Progress Report.
- Li, X., Wu, W., Yu, C.W.F., 2015. Energy demand for hot water supply for indoor environments: problems and perspectives. *Indoor Built Environ.* 24, 5–10.
- Li, K., Lin, B., 2015. Impacts of urbanization and industrialization on energy consumption/CO2 emissions: does the level of development matter? *Renew. Sustain. Energy Rev.* 52, 1107–1122.
- Lin, L., Wang, Z., Xu, Y., Fu, Q., Dong, W., 2018. Larger sensitivity of precipitation extremes to aerosol than greenhouse gas forcing in CMIP5 models. *JGR Atmosphere* 123, 8062–8073.
- Liu, X., Lin, B., Zhang, Y., 2016. Sulfur dioxide emission reduction of power plants in China: current policies and implications. *J. Clean. Prod.* 113, 133–143.
- Liu, B., Duan, Y., Ma, S., Yan, Y., Zhu, C., 2024. Unconventional cold vortex as precursor to historic early summer heatwaves in North China 2023. *NPJ Clim. Atmos. Sci.* 7, 167.
- Lv, A., Fan, L., Zhang, W., 2022. Impact of ENSO events on droughts in China. *Atmosphere* 13, 1764.
- Ma, C., Liu, W., Gou, H., Huang, W., Zhang, R., 2024. Water conservation potential of energy-intensive industries under clean energy and electricity substitution: a case study of nine provinces along the Yellow River Basin. *J. Environ. Manag.* 371, 123256.
- Ma, H., Jing, J., Dai, C., Xu, Y., Qi, P., Song, H., 2025. Spatiotemporal dynamics of drought-flood abrupt alternations and their delayed effects on vegetation growth in Heilongjiang River Basin. *Water* 17 (10), 1419.
- Malhi, Y., Franklin, J., Seddon, N., Solan, M., Turner, M.G., Field, C.B., Knowlton, N., 2020. Climate change and ecosystems: threats, opportunities and solutions. *Phil. Trans. Biol. Sci.* 375, 1–8.
- Meidute-Kavalaiuskiene, I., Davidaviciene, V., Ghorbani, S., Sahebi, I.G., 2021. Optimal allocation of gas resources to different consumption sectors using multi-objective goal programming. *Sustainability* 13, 5663.
- Mi, Z., Sun, X., 2021. Provinces with transitions in industrial structure and energy mix performed best in climate change mitigation in China. *Commun. Earth Environ.* 2, 182.
- Miralles, D.G., Gentine, P., Seneviratne, S.I., Teuling, A.J., 2019. Land-atmospheric feedbacks during droughts and heatwaves: state of the science and current challenges. *Ann. N. Y. Acad. Sci.* 1436, 19–35.
- Mohammadifar, A., Gholami, H., Golzari, S., 2023. Novel integrated modelling based on multiplicative long short-term memory (mLSTM) deep learning model and ensemble multi-criteria decision making (MCDM) models for mapping flood risk. *J. Environ. Manag.* 345, 118838.
- Narayan, P.K., Smyth, R., 2005. Electricity consumption, employment and real income in Australia: evidence from multivariate Granger causality tests. *Energy Policy* 33, 1109–1116.
- Pan, S.-Y., Snyder, S.W., Packman, A.I., Lin, Y.J., Chiang, P.-C., 2018. Cooling water use in thermoelectric power generation and its associated challenges for addressing water-energy nexus. *Water-Energy Nexus* 1, 26–41.
- Pandit, J., Sharma, A.K., 2023. A comprehensive review of climate change's imprint on ecosystems. *J. Water Clim. Change* 14, 4273–4284.

- Pedro-Monzonís, M., Solera, A., Ferrer, J., Estrela, T., Paredes-Arquiola, J., 2015. A review of water scarcity and drought indexes in water resources planning and management. *J. Hydrol.* 527, 482–493.
- Peng, M., Tan, L., Li, H., Wu, J., Ma, T., Xu, H., Xu, J., Zhao, W., Hao, J., 2023. Energy transitions in Yunnan Province based on production function theory. *Energies* 16, 7299.
- Perera, F., 2018. Pollution from fossil-fuel combustion is the leading environmental threat to global pediatric health and equity: solutions exist. *Int. J. Environ. Res. Publ. Health* 15, 16.
- Qi, L., Wang, Y., 2012. Changes in the observed trends in extreme temperatures over China around 1990. *J. Clim.* 25 (15), 5208–5222.
- Qin, N.X., Wang, J.N., Hong, Y., Lu, Q.Q., Huang, J.L., Liu, M.H., Gao, L., 2021. The drought variability based on continuous days without available precipitation in Guizhou Province, Southwest China. *Water* 13 (5), 660.
- Ramanathan, V., Feng, Y., 2009. Air pollution, greenhouse gases and climate change: global and regional perspectives. *Atmos. Environ.* 43, 37–50.
- Saqib, A., Hussain, I., Mefteh-Wali, S., 2024. Do stock returns respond to physical and transition climate risks? Evidence from emerging BRICS economies. *J. Environ. Manag.* 372, 123303.
- Sharma, A., Palwal, K.K., Imoto, S., Miyano, S., 2013. Principal component analysis using QR decomposition. *Int. J. Mach. Learn. Cybernet.* 4, 679–683.
- Shen, L., Wen, J., Zhong, Y., Ullah, S., Cheng, J., Meng, X., 2022. Changes in population exposure to extreme precipitation in the Yangtze River Delta, China. *Climate Services* 27, 100317.
- Sovacool, B.K., Upham, P., Martiskainen, M., Jenkins, K.E.H., Contreras, G.A.T., Simcock, N., 2023. Policy prescriptions to address energy and transport poverty in the United Kingdom. *Nat. Energy* 8, 273–283.
- Sperotto, A., Molina, J.-L., Torresan, S., Critten, A., Marconini, A., 2017. Reviewing Bayesian Networks potentials for climate change impacts assessment and management: a multi-risk perspective. *J. Environ. Manag.* 202, 3020331.
- Srinivasa, A.R., 2012. On the use of the upper triangular (or QR) decomposition for developing constitutive equations for Green-elastic materials. *Int. J. Eng. Sci.* 60, 1–12.
- Sungmin, O., Bastos, A., Reichstein, M., Li, W., Denissen, J., Graefen, H., Orth, R., 2022. The role of climate and vegetation in regulating drought–heat extremes. *J. Clim.* 35, 5677–5685.
- Tan, H., He, Z., Yu, H., Yang, S., Wang, M., Gu, X., Xu, M., 2024. Characterization of extreme rainfall changes and response to temperature changes in Guizhou Province, China. *Sci. Rep.* 14, 20495.
- Tol, R.S.J., 2018. The economic impacts of climate change. *Rev. Environ. Econ. Pol.* 12, 4–25.
- Tumanovskii, A.G., Shvarts, A.L., Somova, E.V., Verbovetskii, E.K., Avrutskii, G.D., Ermakova, S.V., Kalugin, R.N., Lazarev, M.V., 2017. Review of the coal-fired, over-supercritical and ultra-supercritical steam power plants. *Therm. Eng.* 64, 83–96.
- Wang, D., Liu, X., Yang, X., Zhang, Z., Wen, X., Zhao, Y., 2021. China's energy transition Policy expectation and its CO₂ emission reduction effect assessment. *Front. Energy Res.* 8, 627096.
- Wang, X., Liu, R., 2023. The impacts of climate change on the hydrological cycle and water resource management. *Water* 15, 2342.
- Wouters, H., Keune, J., Petrova, I.Y., van Heerwaarden, C.C., Teuling, A.J., Pal, J.S., Vilà-Guerau de Arellano, J., Miralles, D.G., 2022. Soil drought can mitigate deadly heat stress thanks to a reduction of air humidity. *Sci. Adv.* 8, eabe6653.
- Wu, W., Lin, Y., 2022. The impact of rapid urbanization on residential energy consumption in China. *PLoS One* 17, e0270226.
- Xie, S.-P., Miyamoto, A., Zhang, P., Kosaka, Y., Liang, Y., Lutsko, N.J., 2025. What made 2023 and 2024 the hottest years in a row? *NPJ Clim. Atmos. Sci.* 8, 117.
- Yang, J., Tan, C., Wang, S., Wang, S., Yang, Y., Chen, H., 2015. Drought adaptation in the Ningxia Hui autonomous Region, China: actions, planning, pathways and barriers. *Sustainability* 7, 15029–15056.
- Yang, G., Gong, G., Luo, Y., Yang, Y., Gui, Q., 2022. Spatiotemporal characteristics and influencing factors of tourism–urbanization–technology–ecological environment on the yunnan–guizhou–sichuan Region: an uncoordinated coupling perspective. *Int. J. Environ. Res. Publ. Health* 19, 8885.
- Yang, J., Zhao, Z., Fang, W., Ma, Z., Liu, M., Bi, J., 2024. China's progress in synergistic governance of climate change and multiple environmental issues. *PNAS Nexus* 3, pgae351.
- Zhang, K., Luo, J., Peng, J., Zhang, H., Ji, Y., Wang, H., 2022. Analysis of extreme temperature variations on the Yunnan–Guizhou Plateau in Southwestern China over the past 60 years. *Sustainability* 14 (14), 8291.
- Zhang, L., Chu, J., You, H., Liu, Z., 2024. Decomposition and scenario analysis of agricultural carbon emissions in Heilongjiang, China. *PeerJ* 12, e17856.
- Zhao, Y., Wang, S., 2015. The relationship between urbanization, economic growth and energy consumption in China: an econometric perspective analysis. *Sustainability* 7, 5609–5627.
- Zhao, C., Ju, S., Xue, Y., Ren, T., Ji, Y., Chen, X., 2022. China's energy transitions for carbon neutrality: challenges and opportunities. *Carbon Neutral.* 1, 7.
- Zhao, D., Xu, H., Li, Y., Yu, Y., Duan, Y., Xu, X., Chen, L., 2024. Locally opposite responses of the 2023 Beijing–Tianjin–Hebei extreme rainfall event to global anthropogenic warming. *NPJ Clim. Atmos. Sci.* 7, 38.
- Zhong, S., Qian, Y., Zhao, C., Leung, R., Yang, X.-Q., 2015. A case study of urbanization impact on summer precipitation in the Greater Beijing Metropolitan Area: urban heat island versus aerosol effects. *JGR Atmosphere* 120, 10903–10914.
- Zhong, W., Wu, Y., Yang, S., Ma, T., Cai, Q., Liu, Q., 2023. Heavy Southern China Spring rainfall promoted by multi-year El Niño events. *Geophys. Res. Lett.* 50 (7), e2022GL102346.
- Zhuang, F., He, H., Ye, A., Zou, L., 2024. Towards faster and robust solution for dynamic LR and QR factorization. *Sci. Rep.* 14, 27923.
- Zhou, X., Xing, S., Xu, J., Tian, J., Niu, A., Lin, C., 2025. Impacts of climate change risk and economic policy uncertainty on carbon prices: configuration analysis from a complex system perspective. *J. Environ. Manag.* 373, 123622.